Open-File 81-522

UNITED STATES
DEPARTMENT OF INTERIOR
GEOLOGICAL SURVEY

PRELIMINARY GRAVITY INVESTIGATIONS OF THE WAHMONIE SITE, NEVADA TEST SITE, NYE COUNTY, NEVADA

By

David A. Ponce

Open-File Report 81-522

1981

This report is preliminary and has not been reviewed for conformity with U.S. Geological Survey stratigraphic nomenclature. Any use of trade names is for descriptive purposes only and does not imply endorsement by the USGS

Prepared by the U.S. Geological Survey

for the

Nevada Operations Office
U.S. Department of Energy
(Memorandum of Understanding DE-AI08-78ET44802)

Open-File Report 81-522

Open-File Report 81-522

UNITED STATES
DEPARTMENT OF INTERIOR
GEOLOGICAL SURVEY

PRELIMINARY GRAVITY INVESTIGATIONS OF THE WAHMONIE SITE, NEVADA TEST SITE, NYE COUNTY, NEVADA

By

David A. Ponce[1]

[1]U.S. Geological Survey, M/S 18, Menlo Park, California 94025

CONTENTS

ILLUSTRATIONS

TABLES

ABSTRACT

A gravity survey of the southwest corner of the Nevada Test Site was completed during 1979-80 as part of an effort to characterize a possible radioactive waste storage site in granitic rocks. The survey outlined a large, broad, and flat gravity high centered near Wahmonie Site. Combined geophysical data indicate that the anomalous area is underlain by a dense, magnetic, and possibly intrusive body. Gravity data show a +15 milligal Bouguer anomaly coincident with a large positive aeromagnetic anomaly. The data reveal a prominent fault at the west edge of the inferred intrusive. Both gravity and magnetic anomalous highs extend NNE. over a horst composed predominantly of rhyodacite of the Tertiary Salyer Formation. Local aeromagnetic highs are closely associated with two granodiorite exposures on the eastern edge of the horst. A local gravity high of about +2 milligal is centered directly over the southern granodiorite exposure and another high is centered over the northern exposure. A steep gravity gradient outlining the gravity high coincides with the outer edge of a zone of hydrothermal alteration which surrounds the horst. The gravity gradient probably marks the approximate limit of an intrusive body.

INTRODUCTION

A gravity survey of Wahmonie Site was initiated in July 1979 by the USGS (U.S. Geological Survey) as part of an effort to characterize possible radioactive waste storage sites, on behalf of the NVOO (Nevada Operations Office) of the DOE (U.S. Department of Energy).

The specific objectives of the study were to gather regional and detailed gravity data, to present a detailed gravity contour map of the area, and to delineate and interpret the gravity anomaly located near Wahmonie Site. The data presented include: complete Bouguer anomaly maps, residual gravity anomaly maps, and the principal facts for each gravity station.

The interpretation of the gravity anomaly maps was based primarily on existing geologic information, density measurements, and two-dimensional computer modeling. Other unpublished preliminary geophysical data, including aeromagnetic, ground magnetic, seismic refraction, and electrical resistivity methods, were used as supplementary constraints for the interpretation. Gravity models were made along several profiles, including one coincident with a ground magnetic traverse and another coincident with a seismic refraction profile.

The gravity observations were made with LaCoste and Romberg gravity meters G17B and G177. Both meters were periodically checked over gravity meter calibration loops in Nevada (Charleston Peak) and California (Mt. Hamilton). The reduction of the gravity data included removal of the effect of earth tides, instrument drift, latitude correction, free-air correction, Bouguer correction, curvature correction, and the terrain correction to a radial distance of 166.7 km (103.6 mi) for each station.

The purpose of the report is to present the gravity data and the resulting geophysical interpretation of the subsurface structure of Wahmonie Site, and to provide information on the nature and extent of an inferred intrusive granitic body that may be buried beneath Wahmonie Site. This report is part of the geophysical investigations necessary to evaluate Wahmonie Site as a possible nuclear waste repository in granitic rocks at the NTS (Nevada Test Site).

ACKNOWLEDGMENTS

I appreciate the assistance of H. M. VanBuren in planning and coordinating part of the field work and of R. N. Harris, D. C. Hohbach, E. G. Miller, and J. B. Spielman for assisting in the gravity observations, elevation control, terrain corrections, and map digitization. G. D. Bath, D. L. Healey, J. H. Healy, D. B. Hoover, and L. W. Pankratz provided preliminary geophysical data or interpretations. H. W. Oliver gave timely suggestions, guidance, and supervision of the project. J. P. Brooke, R. S. Creely, G. L. Dixon, and Donald Plouff gave critical reviews and suggestions.

LOCATION

The study area lies within the Skull Mountain 7½ minute quadrangle and is located on the NTS, southern Nye County, Nevada (fig. 1). The study area includes most of Area 26 and parts of Area 6, 14, 25, 27, 28, 29, and 401 (fig. 2). The NTS is about 112 km (70 mi) WNW. of Las Vegas along U.S. Highway 95 (fig. 3). The NTS has about 3,500 km^2 (1,350 mi^2) of controlled area and is adjacent to the Nellis Air Force Bombing and Gunnery Range. Public access to the NTS is not permitted. However, once security checks are obtained, the study area is easily accessible (fig. 2). Mercury Highway, a 2-lane paved road, connects U.S. Highway 95 to Mercury and the forward areas of NTS. Cane Spring Road, a 2-lane paved road, branches from Mercury Highway and bisects the study area into north and south halves. Numerous but seldom used jeep trails intersect Cane Spring Road and quickly become rugged. Four-wheel drive vehicles with high ground clearance are recommended.

TOPOGRAPHY AND HYDROLOGY

The topography and drainage of the NTS area are typical of the Basin and Range province where closed basins are separated by ranges, hills, and mesas. There are three prominent intermontane valleys at the NTS: Jackass Flats, Frenchman Flat, and Yucca Flat (fig. 3). In the study area (plate 1), Jackass Flats ranges in elevation from about 790 m (2,600 ft) to 980 m (3,200 ft). Mountain ranges typically rise 610 m (2,000 ft) to 910 m (3,000 ft) above the basins. The two highest peaks in the study area, Skull Mountain to the south and Lookout Peak to the north, rise to 1,821 m (5,975 ft) and 1,722 m (5,651 ft),

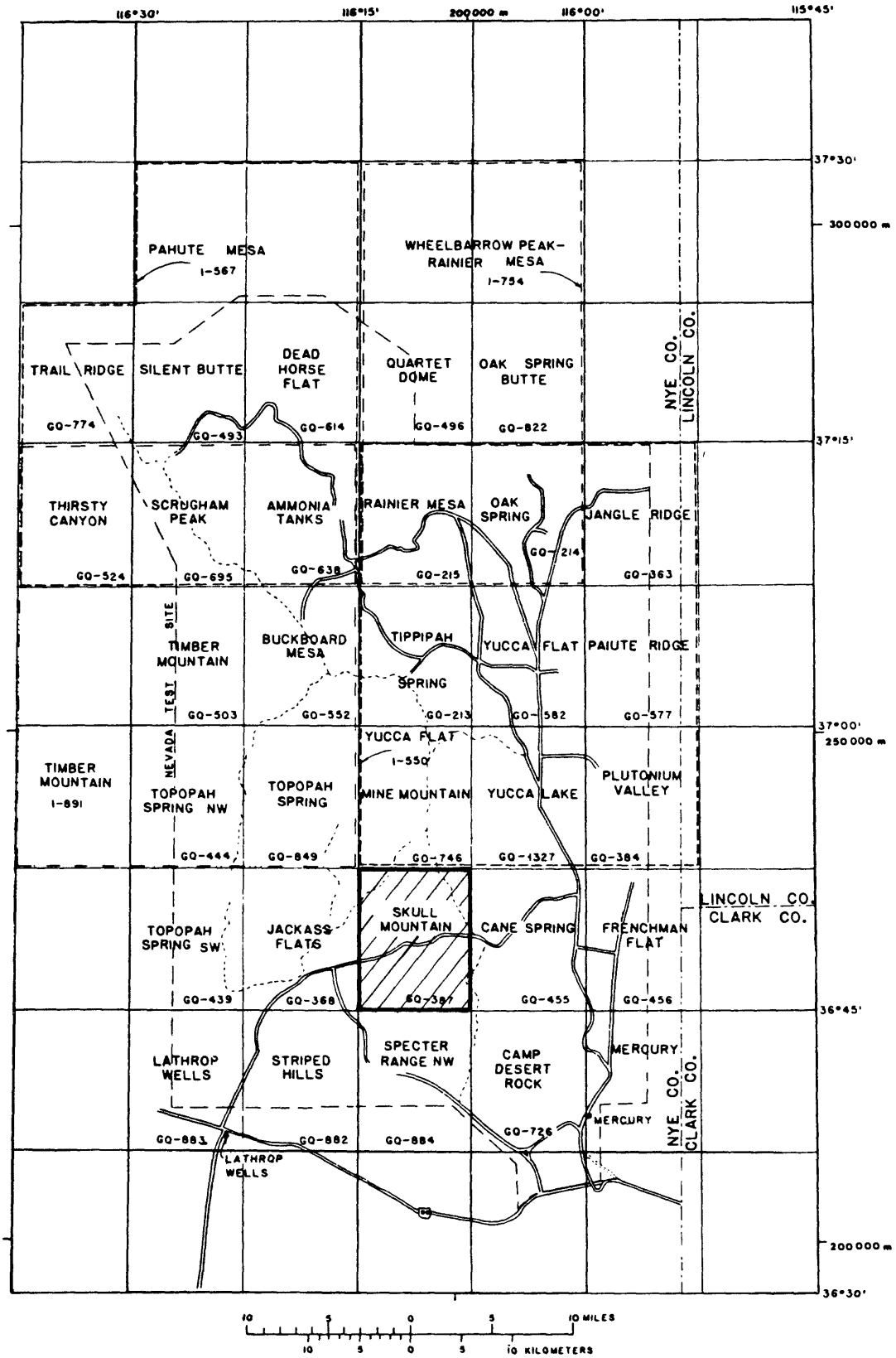

Figure 1.--Index map of the Nevada Test Site showing the outlines of geologic maps and the location of the study area (ruled area).

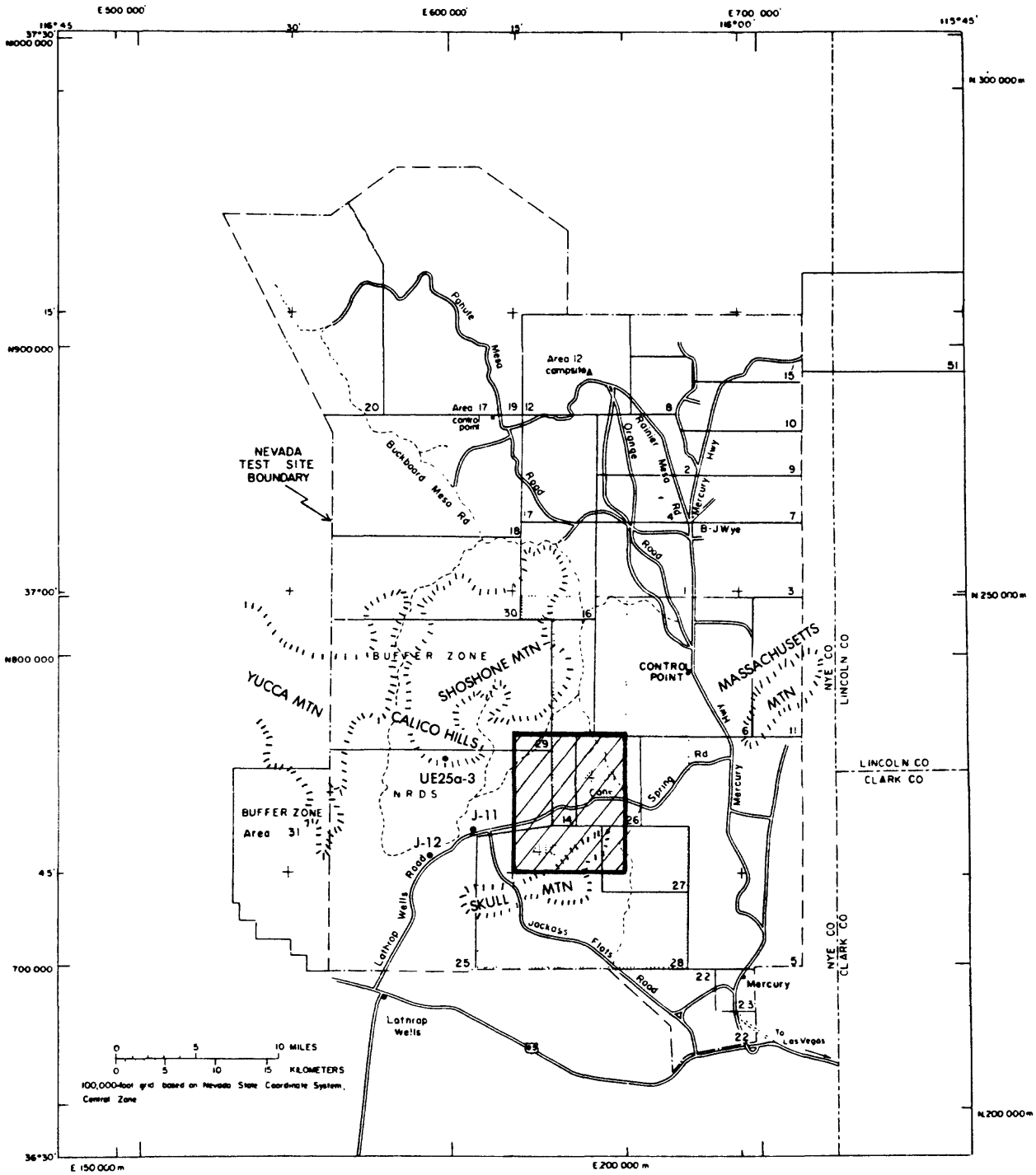

Figure 2.--Index map of the Nevada Test Site showing the outlines of numbered test areas and the location of the study area (ruled area).

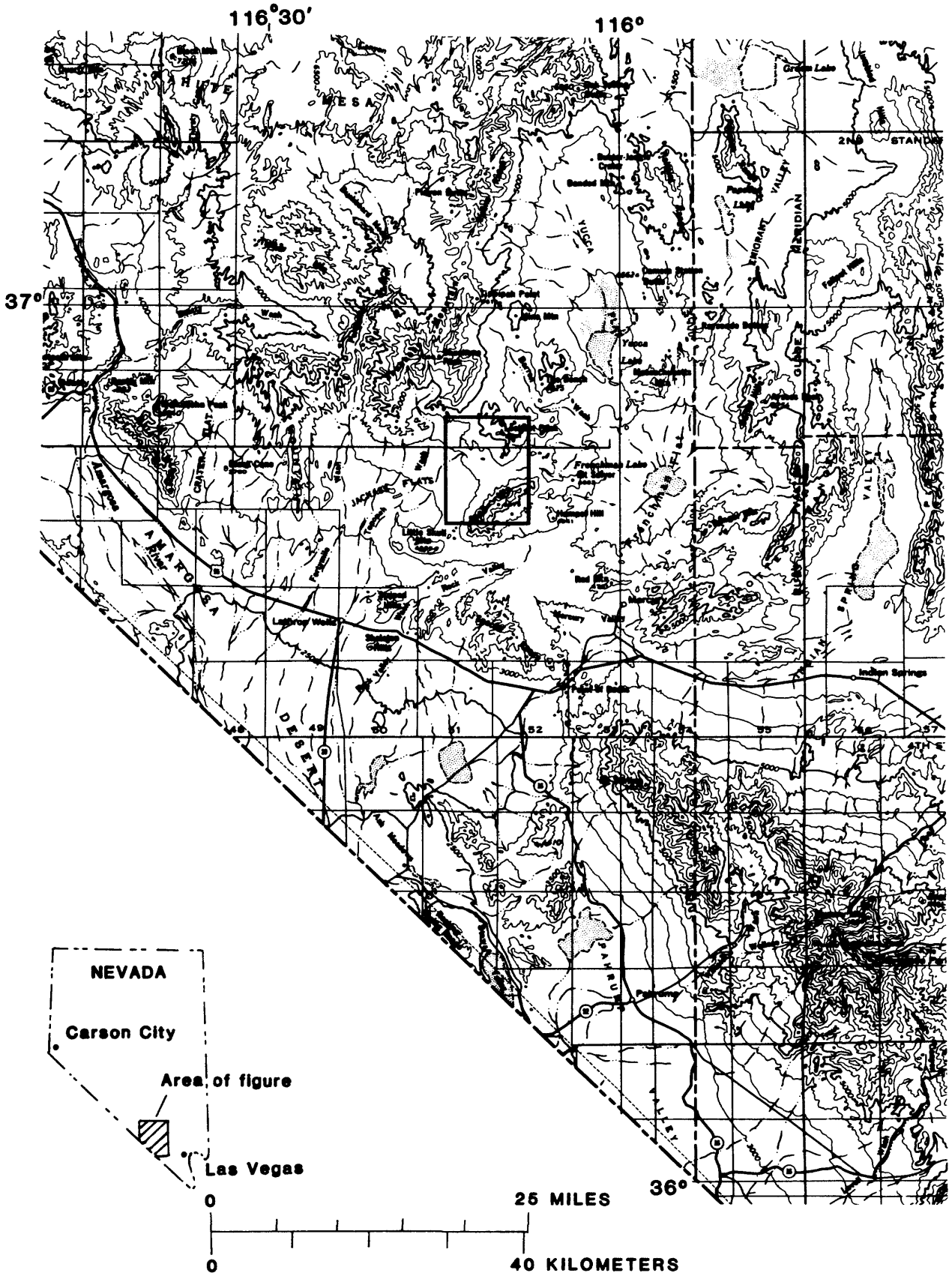

Figure 3.--Index map of a part of southern Nevada showing the location of the study area.

respectively. Kiwi Mesa, a prominent feature of the Skull Mountain quadrangle, rises 610 m (2,000 ft) above Jackass Flats to an elevation of 1,500 m (4,900 ft). North of the Horn Silver mine, a prominent ridge trending N.10°E. rises as much as 323 m (1,062 ft) from the low drainage divide between east Jackass Flats and Wahmonie Flat.

Drainage in the NTS area is primarily by the subsurface flow of ground water. Water flows both through the alluvium and along fractures in Paleozoic carbonate rocks that underlie the basins and intervening ranges. Winograd (1962) presented evidence for the interbasin circulation of ground water through carbonate rocks of Paleozoic age at the NTS, including the three large intermontane valleys of Jackass Flats, Frenchman Flat, and Yucca Flat. Eakin and others (1963, p. 23) found that available water-table altitudes for wells in the three larger basins of the NTS were enough alike that hydraulic connection between the basins, as opposed to separation, seemed more probable.

Ground water in the valley fill and Tertiary volcanic rocks at Yucca Flat are draining into the underlying Paleozoic carbonate rocks (Winograd, 1962, p. 44). Ground water in these Paleozoic rocks flows southwestward toward Ash Meadows in the Amargosa Desert (fig. 3). Jackass Flats and the Amargosa Desert are also connected hydrologically by the flow of ground water through highly fractured carbonate aquifers which underlie and flank the basin and through welded tuffs which occur in the upper part of the Tertiary volcanic rock sequence. The welded tuff aquifer is a major source of water supply in Jackass Flats. In other areas of the NTS the welded tuff appears to be an aquitard. The welded tuffs appear to be a source of water only in structurally deep intermontane basins, where they occur within the zone of saturation (Winograd and Thordarson, 1979, p. C31). Similar to the carbonate aquifers, these strata transmit water primarily through fractures and have a wide range in transmissibility from 280 to 120,000 gpd (gallons per day) per foot, with a median of 3,700 gpd per foot (Winograd, 1962, p. 29).

The static water level in two wells in Jackass Flats is about 730 m (2,400 ft) above sea level (table 1). Well J-11 has a static water level 316 m (1,037 ft) below the surface and an alluvial thickness of 312 m (1,025 ft). Well J-12 has a ground water level at 226 m (741 ft) below the surface with an alluvial thickness of 157 m (515 ft). (See Moore, 1962, p. 27-34.)

Although the regional water table in Wahmonie Flat is at a depth of 518 m (1,700 ft), perched water occurs throughout most of Area 401 in eastern Wahmonie Flat (Johnson and Ege, 1964, p. 19). Water levels in eastern Wahmonie Flat are summarized in table 2.

Table 1.--Water-levels in Jackass Flats, Nevada Test Site[1]

Well	Depth of Well (ft)	Water-Table Depth (ft)	Water-Table Altitude (ft)	Alluvial Thickness (ft)
J-11	1,329	1,037.5	2,407	1,025
J-12	887	741.4	2,387	515

[1]Modified from Moore (1962, p. 27-34).

Table 2.--Water-levels averaged over a six-day period in Area 401, Wahmonie Flat, Nevada Test Site[1]

Drill Hole	Elevation of Drill Hole (ft)	Water-Table Depth (ft)	Water-Table Altitude (ft)
Pluto-4	4,152	109	4,042
-5	4,041	81	3,960
-6	4,091	167	3,924
-7	4,091	159	3,932
-10	4,060	129	3,931
-11	4,060	126	3,934
-12	4,060	128	3,932

[1]Modified from Johnson and Ege (1964, p. 20).

GEOLOGY

General

The NTS lies near one of the thickest parts of the Paleozoic Cordilleran miogeosynclinal section. Alluvial basins constitute about 30 percent of the area, upper Paleozoic and uppermost Precambrian sedimentary rocks form approximately 30 percent of the outcrops, and the remainder consists primarily of Tertiary volcanic and intrusive rocks (Ekren, 1968, p. 11). Ball (1907) reported a geologic reconnaissance of part of southern Nevada and eastern California which now include parts of the NTS. Johnson and Hibbard (1957) recognized 17 Paleozoic formations and one of Tertiary age at the NTS. Their Tertiary Oak Spring Formation was later divided, raised to the rank of Group, and the term finally abandoned (Orkild ,1965, p. A44).

The Paleozoic formations are Early Cambrian to Early Permian and consist of miogeosynclinal shallow-water deposits including limestone, dolomite, quartzite, shale, and conglomerate. Uppermost Paleozoic and Precambrian sedimentary rocks have nearly 12,200 m (40,000 ft) of exposed thickness (Ekren, 1968, p. 12).

The Mesozoic Era is represented by scattered granitic plutons including the Climax, Gold Meadows, and Twinridge stocks which crop out in the NE. section of the NTS. Six biotite samples from the quartz monzonite of the Climax stock yielded an average K-Ar date of 93 m.y. (Cornwall, 1972, p 14). The age of quartz monzonite from the Gold Meadows stock, determined by K-Ar, is 91.8 $\pm$ 2.6 m.y. (Cornwall, 1972, p. 14).

Tertiary rocks of the NTS consist predominantly of ash-fall and ash-flow tuffs. (See Ross and Smith, 1961, p. 3-8, for definition of terms.) The tuffs are dominantly rhyolitic in composition and range in age from 26 to 7 m.y. The Tertiary volcanic rocks are represented by a composite section more than 9,000 m (30,000 ft) thick (Ekren, 1968, p. 13-14).

Wahmonie Site Geology

A generalized geologic map of the Skull Mountain quadrangle modified from the geologic map of Ekren and Sargent (1965), is shown in figure 4. Most of the Tertiary volcanic rocks have been combined into one unit. The-site specific geology includes the horst (hereafter referred to as the Wahmonie horst) trending NNE. and the immediately surrounding area. The horst is about 1.6 km (1 mi) wide, about 4.8 km

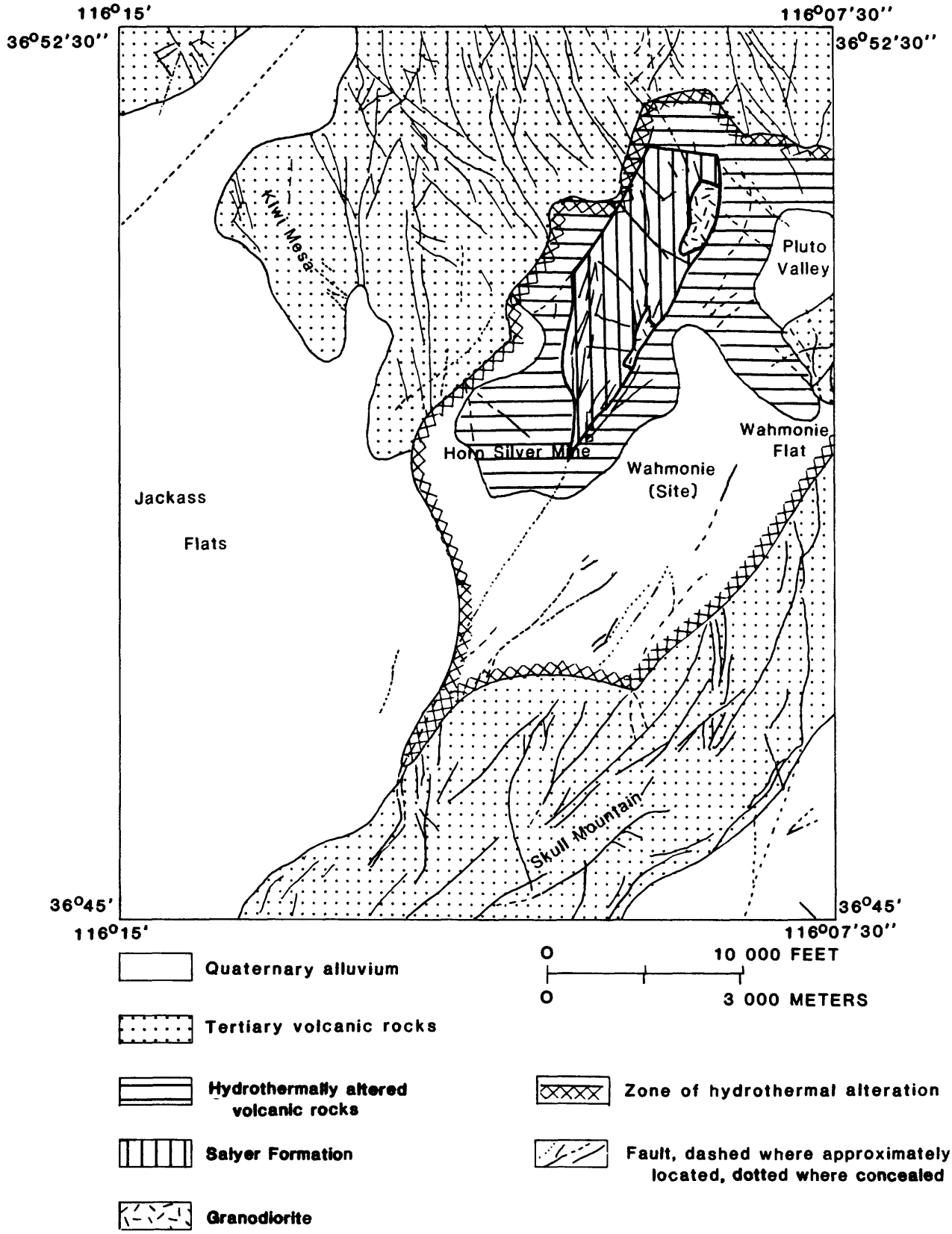

Figure 4.--Generalized geologic map of the Skull Mountain 7½' quadrangle (After Ekren and Sargent, 1965).

(3 mi) in length, and is predominantly composed of rhyodacite of the Late Miocene Salyer Formation. Two Tertiary granodiorite intrusive bodies occur along the eastern margin of the Wahmonie horst. The northern granodiorite body is closely associated with and nearly encircles a small outcrop of the Eleana Formation of Carboniferous age (plate 1) which may be a roof pendant. The Eleana outcrop consists of light-green to tan quartzite, calcareous sandstone, and conglomerate (Ekren and Sargent, 1965). Other, smaller intrusive bodies are present within the horst and are composed of andesite, rhyolite, and intrusive breccia.

The Wahmonie horst is completely surrounded by a zone of hydrothermally altered Tertiary volcanic rocks of the Wahmonie Formation; these rocks include altered andesite, dacite, latite, and tuff that are difficult to distinguish megascopically.

Salyer and Wahmonie Formations

The Tertiary Salyer and Wahmonie Formations are composed of a series of lava flows, volcanic breccia, tuff, and sandstone. The Salyer Formation, which exceeds 700 km^2 (300 mi^2) in extent, is centered near Mt. Salyer and Cane Spring in the Cane Spring quadrangle (fig. 10), has a maximum thickness of 600 m (2,000 ft), and a volume of 80 km^3 (20 mi^3). The Wahmonie Formation overlies the Salyer Formation, has an areal extent exceeding 1,300 km^2 (500 mi^2) near its type area in Wahmonie Flat, a maximum thickness of 1,100 m (3,500 ft), and a volume of about 100 km^3 (25 mi^3). (See Cornwall, 1972, p. 23.)

Rocks of the Wahmonie Formation are generally more mafic, contain primary hornblende, are less altered, and consist mainly of lava flows and related tuffs. Rocks of the Salyer Formation are more acidic, contain primary pyroxene and secondary hornblende, are more altered, and consist of breccia flows, interstratified tuff, sandstone, and volcanic breccia. Chemically, the Wahmonie Formation ranges from rhyodacite to dacite whereas the Salyer Formation is dellenitic to rhyodacitic in composition. The chemical and mineralogic similarities of the two formations indicate that they are comagmatic. (See Poole and others, 1964, p. A43.) Rocks of the Wahmonie and Salyer Formations are probably genetically related to the volcanic assemblages in the Wahmonie horst (plate 1) and are believed to be extrusive equivalents of the granodiorite (G. L. Dixon, oral commun., 1980).

The lower and upper parts of the Wahmonie Formation have been dated by Kistler (1968, p. 255), at 12.9 and 12.5 m.y., respectively using the potassium-argon method. The Salyer Formation is older and is Late Miocene.

STRUCTURE

The principal structures at the NTS include thrust faults, concentric and radial faults associated with doming in volcanic centers, high-angle normal faults related to Basin and Range faulting, and strike-slip faults. Ekren and others (1968, p. 247) recognize two systems of faulting at the NTS. The earlier system consists of two sets, one striking northeast and the other striking northwest. The earlier set is developed only in rocks older than 17 m.y. The younger system strikes north and cuts 14 m.y. old tuff that is not cut by the older system. The north-trending faults thus developed between 17 and 14 m.y. ago. In the southern part of the NTS, north-trending faults gradually change strike to the northeast. The change in strike is believed to be caused by drag due to the right-lateral movement along the Las Vegas Valley shear zone (Ekren and others, 1968, p. 247).

There are two prominent fault trends in the study area. Steep-angle normal-faults trend NNW. in the northernmost part of the area, whereas faults bounding the Wahmonie horst and those within Skull Mountain trend NNE. Faulting within the horst generally trends NNW. and is most intense in the rhyodacite rocks of the Salyer Formation (plate 1).

Rhyodacite rocks of the horst show flow layering with dips generally ranging from 20° to 40°. Several folds outlined by flow layering in the basalt of Kiwi Mesa and the dacitic flows of Skull Mountain probably reflect the underlying topography (Ekren and Sargent, 1965).

MINERAL RESOURCES

The Wahmonie mining district is located in the Skull Mountain 7½ minute quadrangle, about 3 km (2 mi) north of Skull Mountain, near the low drainage divide between Jackass Flats and Wahmonie Flat (plate 1). Mineralization at the Horn Silver mine occurs along quartz viens and seams associated with shear zones in the hydrothermally altered andesites, latites, dacites, and tuffs of Wahmonie Flat. Exploration at the Horn Silver mine began before 1905 (Ball, 1907, p. 140). The district was later rediscovered with a strike of high-grade silver-gold ore, by McRea and Lefler in 1928. An Engineering and Mining Journal of that time carried an article stating that about 3 weeks after the strike, Wahmonie Camp had a population of about 200. Although only minor shipments of ore were made, the Wingfield interests sank a 150-meter (500-foot) vertical shaft at the Horn Silver mine. In 1951, the

Wahmonie property was held by location by C. M. Dubois of Los Angeles, Calif., who stated that $32 ore was found on the 20-meter (65-foot) level. (See Kral, 1951, p. 206-207.)

Recent geophysical exploration including VES (vertical electrical soundings) and IP (induced potential) methods indicate that the Wahmonie district would make an attractive minerals exploration target (D. B.Hoover, written commun., 1980).

GRAVITY METHODS

General

Standard gravity corrections were used on the data gathered during the field survey, similar to those used in commercial gravity reduction methods (Dobrin, 1960, p. 188). The corrections include: (a) the earth-tide correction, which removes the effect of the tidal attraction of the sun and moon, (b) the instrument drift correction, (c) the free-air correction, which accounts for the fact that each station is at a different elevation, (d) the Bouguer correction, which accounts for the attraction of rock material between the station and sea level, (e) the latitude correction, which takes into account the variation of the earth's gravity at sea level, (f) the curvature correction, which corrects the Bouguer correction for the effect of the earth's curvature to 166.7 km (103.6 mi), and (g) the terrain correction, which removes the effect of topography to a radial distance of 166.7 km (103.6 mi).

LaCoste and Romberg gravity meters G17B and G177, with calibration factors of 1.00252 and 1.0003, respectively, were used in the gravity survey. Both meters were periodically checked on calibration loops in Nevada (Charleston Peak) and California (Mt. Hamilton) prior to and after the field survey. The meters were run together on most of the detailed stations in the study area. All gravity data obtained in the survey were reduced using the Geodetic Reference System of 1967 (International Union of Geodesy and Geophysics, 1971) and referenced to the IGSN 1971 gravity datum (Morelli, 1974, p. 18) by means of base stations tied to the IGSN gravity datum at Indian Springs and Las Vegas, Nev.

Elevation Control

All gravity readings were made on bench marks, at photogrammetric "spot" elevations, or on surveyed points. Photogrammetric spot

elevations are considered accurate to within ± ½ of the 6-meter (20-foot) contour interval or ±3 m (10 ft). A 3-meter (10-foot) uncertainty in elevation results in a Bouguer anomaly uncertainty of 0.6 mGal, a value which is well below the allowable error for most regional gravity work. All detailed gravity stations were surveyed using an electronic distance-measuring instrument that transmits a modulated infrared light beam to a retro-flector target, which sends the beam back to the instrument. The phase shift between the transmitted and received signals is proportional to the slope distance being measured. The instrument is capable of measuring slope distance and zenith angle simultaneously and then calculating horizontal and vertical distances automatically. The detailed stations were surveyed by employees of the USGS and are believed accurate to within ±0.1 m (±0.3 ft) vertically from a reference bench mark.

Terrain Corrections

The terrain correction removes the effect of material higher than the gravity station and the effect of material needed to fill in any valleys below the station. Because the attraction of material at an elevation higher than the station has an upward vertical component that is opposite to the earth's gravity, its effect is removed by adding the correction to the observed gravity value. The effect of rock material needed to fill in valleys below the station has already been subtracted in the calculation of the Bouguer correction. The attraction of this material must be added to the observed gravity to restore what was subtracted in the Bouguer correction. Thus, the terrain correction is always added to the observed gravity whether the topographic feature is above or below the station. (See Dobrin, 1960, p. 189.)

The terrain correction procedure used in the reduction of the gravity data is similar to that discussed by Robbins and others (1974), in which manual corrections were computed to a radial distance of 0.59 km (0.37 mi) (outer radius of the Hayford zone "D") from each gravity station and extended by digitization and computer analysis to a radial distance of 166.7 km (103.6 mi).

The Hayford-Bowie "AB" zone extends to a radial distance of 68 m (223 ft) from the gravity station. Since topographic maps do not show the detail needed this close to a station, terrain corrections for the AB zone were estimated in the field with the aid of tables and charts. The few stations that weren't easily calculated in the field were sketched and later calculated in the office by more complex methods outlined by Dobrin (1960, p. 171-178) and Nettleton (1942, p. 102-127).

The "C" and "D" zone corrections were calculated by averaging compartment elevations on a circular template based on Hayford's system of zones (Swick, 1942, p. 66). Several modifications to make the system

faster and more accurate were made by S. L. Robbins and others (1974, p. 4) including extended and recomputated terrain correction tables, and a system of subzones.

The terrain correction for each station from a radial distance of 0.59 km (0.37 mi) to 166.7 km (103.6 mi), was made using a computer program by Plouff (1966, 1977) that is based on a grid of geographic coordinates where average elevations are digitized from topographic maps. Corrections for the radial distance from 0.59 km (0.37 mi) to 2.0 km (1.2 mi) use average digitized elevations of 1/4 x 1/4 minute compartments, corrections from 2.0 km (1.2 mi) to 5.00 km (3.1 mi) use 1/2 x 1/2 minute compartments, corrections from 5.0 km (3.1 mi) to 20.0 km (12.4 mi) use 1 x 1 minute compartments, and corrections from 20.0 km (12.4 mi) to 166.7 km (103.6 mi) use 3 x 3 minute compartments.

BULK DENSITY

Hazelwood (1963, p. 25-26) separates rock densities at the Nevada Test Site into three groups; the first group consists of Precambrian and Paleozoic rocks that range in density from 2.49 to 2.85 g/cm^3 and average 2.67 g/cm^3. The second group is composed of Cenozoic volcanic rocks that range from 1.78 to 2.87 g/cm^3 and average about 2.40 g/cm^3. The third group consists of nonwelded and partially welded ash-flow tuffs and alluvium and average about 2.00 g/cm^3. Densities of rock samples from the NTS are summarized in table 3.

Paleozoic rocks of the Eleana Formation are exposed in the northeast edge of the Wahmonie horst and are limited in areal extent. Seven meta-sediment samples, mapped as the Eleana Formation, range in density from 2.98 to 3.18 g/cm^3 and average of 3.12 g/cm^3. X-ray diffraction analysis shows that these rocks are composed predominantly of diopside, a calcium-rich pyroxene that ranges in density from 3.2 to 3.3 g/cm^3. Two samples of light-tan quartzite samples of the Eleana Formation in the Wahmonie horst have densities of 2.58 to 2.63 g/cm^3 with an average of 2.61 g/cm^3. Other Paleozoic rocks, from Yucca Valley and Area 9 (figs. 2,3), have mean bulk densities of 2.65 and 2.63 g/cm^3, respectively. Twenty core samples from drill hole UE25a-3 (fig. 2) average 2.54 g/cm^3 for an altered argillite interval of the Eleana Formation (Maldonado and others, 1980, p. 38). Twenty-three samples of Tertiary granodiorite from the Wahmonie horst have a mean bulk density of 2.65 g/cm^3 with a range of 2.60 to 2.69 g/cm^3. Although considerably younger, the Tertiary granodiorite is very similar to the Mesozoic Climax stock granodiorite in Area 15 (fig. 2), in which 3 samples have a density of 2.64 g/cm^3 and 15 samples have a density range of 2.61 to 2.69 g/cm^3 with an average of 2.68 g/cm^3.

Eight samples of intrusive blue-gray to black andesite from the Wahmonie horst range in density from 2.62 to 2.70 g/cm^3 and average of 2.66 g/cm^3. Rhyodacite of the Salyer Formation, which constitutes most of the Wahmonie horst, ranges in bulk density from 2.53 to 2.65 g/cm^3 and averages 2.59 g/cm^3. Eighteen samples of hydrothermally altered rock of the Wahmonie Formation have a mean bulk density of 2.36 g/cm^3. Samples of dacite porphyry from the Wahmonie Formation from five drill cores in eastern Wahmonie Flat, Area 401 on the Cane Spring quadrangle (figs. 2, 8) range in dry bulk density from 1.35 to 2.55 g/cm^3 and average 2.27 g/cm^3, and show a range in grain density from 2.17 to 2.63 g/cm^3 with an average of 2.54 g/cm^3. Dacite porphyry of the Wahmonie Formation from drill hole Pluto-1 in eastern Wahmonie Flat ranges in dry bulk density from 1.81 to 2.43 g/cm^3 and averages 2.27 g/cm^3. Tertiary volcanic rocks from the Massachusetts Mountain (fig. 2) and Mt. Salyer (fig. 8) areas range in bulk density from 1.55 to 2.71 g/cm^3 and average 2.22 g/cm^3.

Borehole gravity meter studies by Healey (1967, p. 1) show that the Rainier Mesa Member of the Timber Mountain Tuff ranges in density from 2.03 to 2.22 g/cm^3 and averages 2.13 g/cm^3, and the Painbrush Tuff ranges from 1.49 to 1.70 g/cm^3 and averages of 1.58 g/cm^3. Rock samples from the Rainier Mesa member show good agreement with the borehole gravity data with an average dry bulk density of 2.18 g/cm^3 and an average grain density of 2.55 g/cm^3. Seventy-six rock specimens from the Paintbrush Tuff also corroborate the borehole gravity data with an average dry bulk density of 1.50 g/cm^3 and a grain density of 2.33 g/cm^3. The welded tuff of the Rainier Mesa member has an appreciably higher bulk and grain density than non-welded tuffs.

Thirty-three samples of Quaternary alluvium have a wide range in densities, from 1.30 to 2.12 g/cm^3, partly dependent on the lithology of the source rocks. Density log data from drill hole Ue11c in northern Frenchman Flat average 2.05 g/cm^3 for 460 m (1,500 ft) of alluvium (Carr and others, 1975, p. 17).

Table 3.--Mean bulk densities of rock specimens at the Nevada Test Site

Lithology	Number of samples	Mean bulk density (g/cm^3)	Range of density	Remarks
Quaternary				
Alluvium[1]	10	1.92	1.81-2.12	N. Yucca Valley.
Do[2]	7	1.46	1.30-1.81	Yucca Valley, Jangle area.
Do[2]	14	1.65	1.30-1.81	Do.
Do[3]	2	1.58	1.54-1.62	S. Yucca Flat.
Tertiary				
Andesite	8	2.66	2.62-2.70	Wahmonie horst.
Breccia flow	6	2.58	2.54-2.60	Salyer Fm.
Breccia flow, altered	6	2.31	2.21-2.49	Do.
Dacite porphyry[4]	81	2.27	1.33-2.55	Wahmonie Fm.
Dacite porphyry[4]	76	2.27	1.81-2.43	Do.
Granodiorite	23	2.65	2.60-2.69	Wahmonie horst.
Hydrothermally altered rock	18	2.36	2.17-2.50	Wahmonie Fm.
Paintbrush Tuff[6]	76	1.50	n.a.[6]	Area 12.
Rhyodacite	11	2.59	2.53-2.65	Salyer Fm.
Tuff, Rainier Mesa Member[5]	31	2.18	n.a.	Area 12.
Volcanic rocks[7]	77	2.22	1.55-2.71	Massachusetts Mtn. and Mt. Salyer areas.
Mesozoic				
Granodiorite[8]	15	2.68	2.61-2.69	Climax Stock.
Do[3]	3	2.64	2.64	Do.
Paleozoic				
Argillite[1]	n.a.	2.65	n.a.	Yucca Valley.
Limestone[3]	3	2.63	2.62-2.65	Area 9.
Meta-sediment	7	3.12	2.98-3.18	Wahmonie horst.
Quartzite	2	2.61	2.58-2.63	Do.

[1]Healey and Miller (1962, p. 11).
[2]Diment and others (1959, p. 7).
[3]Barnes (1967, p. 7-15).
[4]Johnson and Ege (1967, p. 38-40).
[5]Keller (1959, p. 3-5).
[6]Not available.
[7]Carr and others (1975, p. 17).
[8]Izett (1960, p. 10).

AEROMAGNETIC DATA

A generalized aeromagnetic map, modified from the aeromagnetic map of the Skull Mountain quadrangle (U.S. Geological Survey, 1979), is shown in figure 5. The survey was flown 120 m (400 ft) above the ground surface (drape). There are two prominent aeromagnetic trends in the study area. The northeast trend in the southern half of the map consists of a series of linear anomalies that are directly associated with the rocks of Skull Mountain (fig. 5). These rocks include several of the anomaly-producing units described by Bath (1968, p. 139), including the Topopah Spring member of the Paintbrush Tuff and the Rainier Mesa and Ammonia Tanks Members of the Timber Mountain Tuff. The more prominent of the two magnetic features is a large magnetic high centered near Wahmonie Site. This anomaly has a magnetic prominence extending northward along the eastern margin of the Wahmonie horst. Two smaller oval-shaped closed highs located along the eastern edge of the horst directly correlate with two small granodiorite outcrops. This correlation suggests that the larger anomaly may also be associated with a granitic body buried near the surface at Wahmonie Site. A local magnetic high directly overlies Kiwi Mesa (fig. 4) in the NW. corner of the study area. The magnetic high appears to be associated with the Kiwi Mesa basalt which has an outcrop thickness of about 76 m (250 ft).

GRAVITY INTERPRETATION

Bouguer Gravity

The complete Bouguer anomaly map of the study area, reduced for a density of 2.67 g/cm^3, is shown in figure 6. Bouguer anomaly values range from -154 mGal along the northern edge to a high of -135 mGal near the center of the quadrangle. The large negative values suggest isostatic compensation and are typical of continental masses where an inverse relation between anomaly and elevation generally exists. Gravity values rapidly decrease southward along the foot of Skull Mountain reflecting a too-high reduction density for the Tertiary volcanic rocks that form Skull Mountain. Tertiary rock samples (table 3) suggest that a better estimate for the density of Skull Mountain is 2.00 to 2.20 g/cm^3. This estimate is corroborated by the partial elimination of the anomalous low when using the lower reduction density of 2.30 g/cm^3 (fig. 7). Except for the anomalous low associated with Skull Mountain, the shape of the major features of figure 6 are only slightly modified by the lower reduction density. This can be seen over

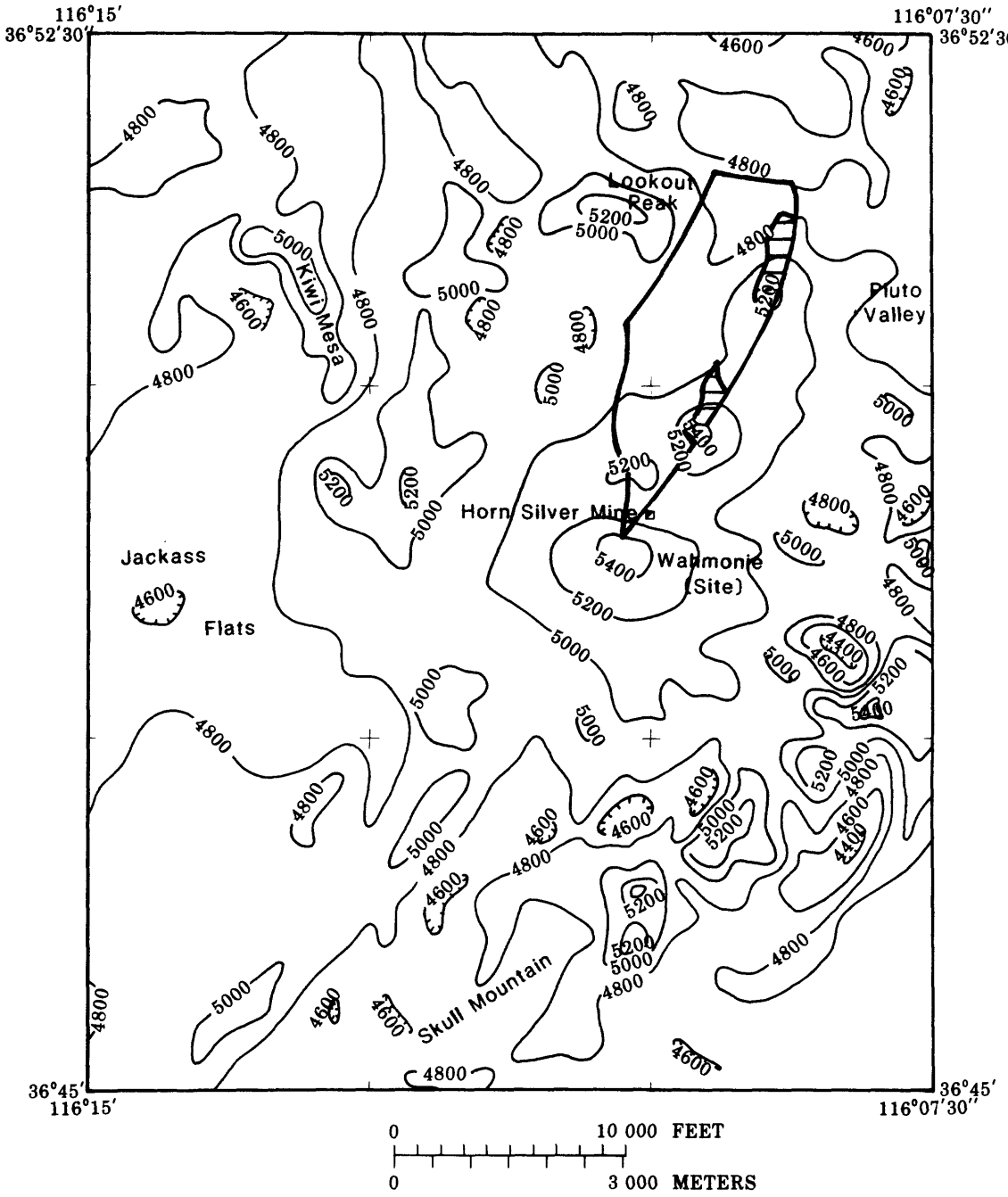

Figure 5.--Residual aeromagnetic map of the Skull Mountain 7½' quadrangle. The Wahmonie horst is outlined. Granodiorite exposures are shown as ruled areas. Magnetic lows are hachured. The contour interval is 200 gammas. The flight elevation is 400-ft drape. Flight lines have 1/4-mi east-west spacings. Corrected for IGRF 1975 with a 5,000-gamma constant added.

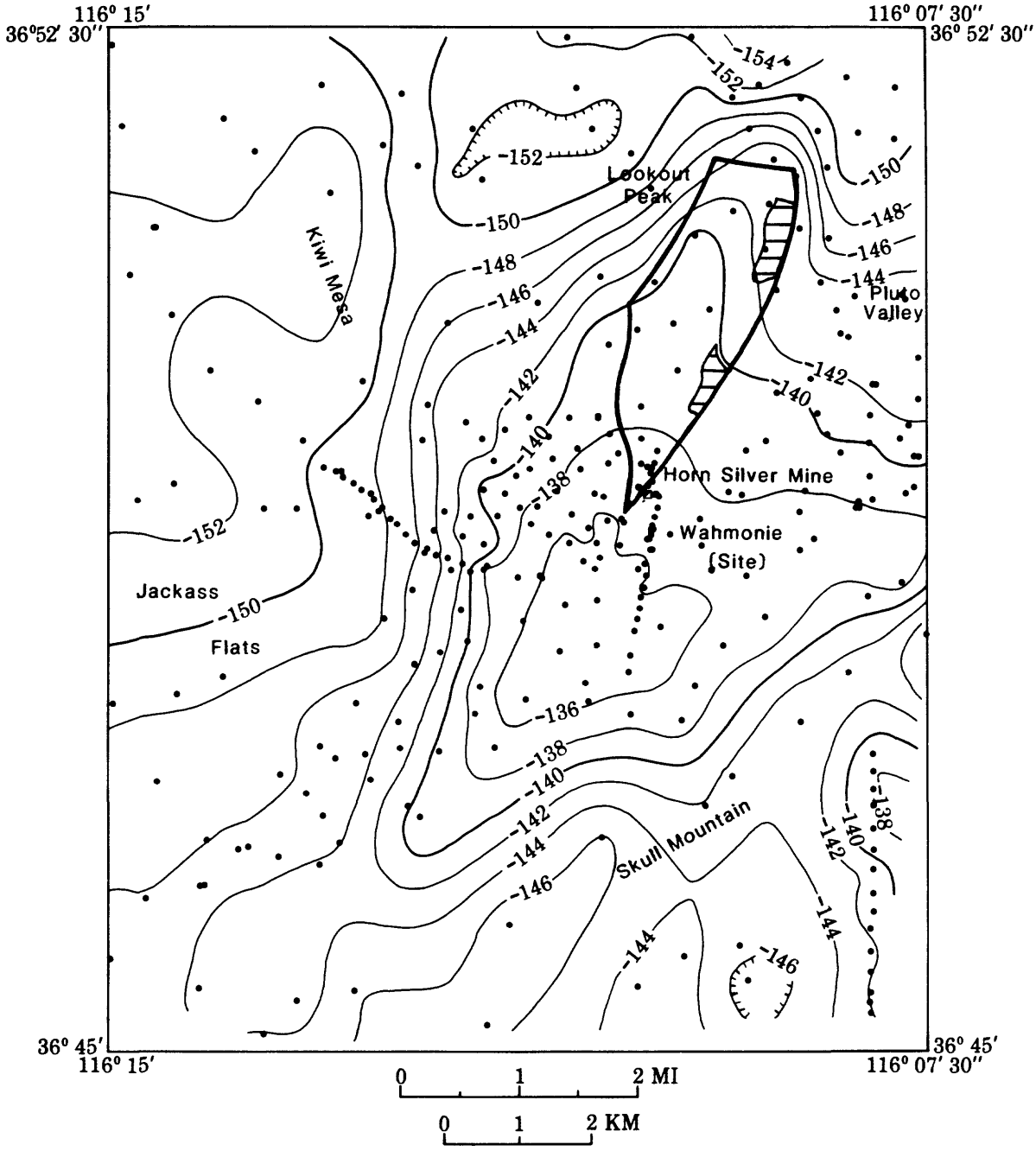

Figure 6.--Complete Bouguer anomaly contour map of the Skull Mountain 7½' quadrangle reduced for a density of 2.67 g/cm^3. The contour interval is 2 mGal. The Wahmonie horst is outlined. Granodiorite exposures are shown as ruled areas. Hachures indicate closed gravity lows.

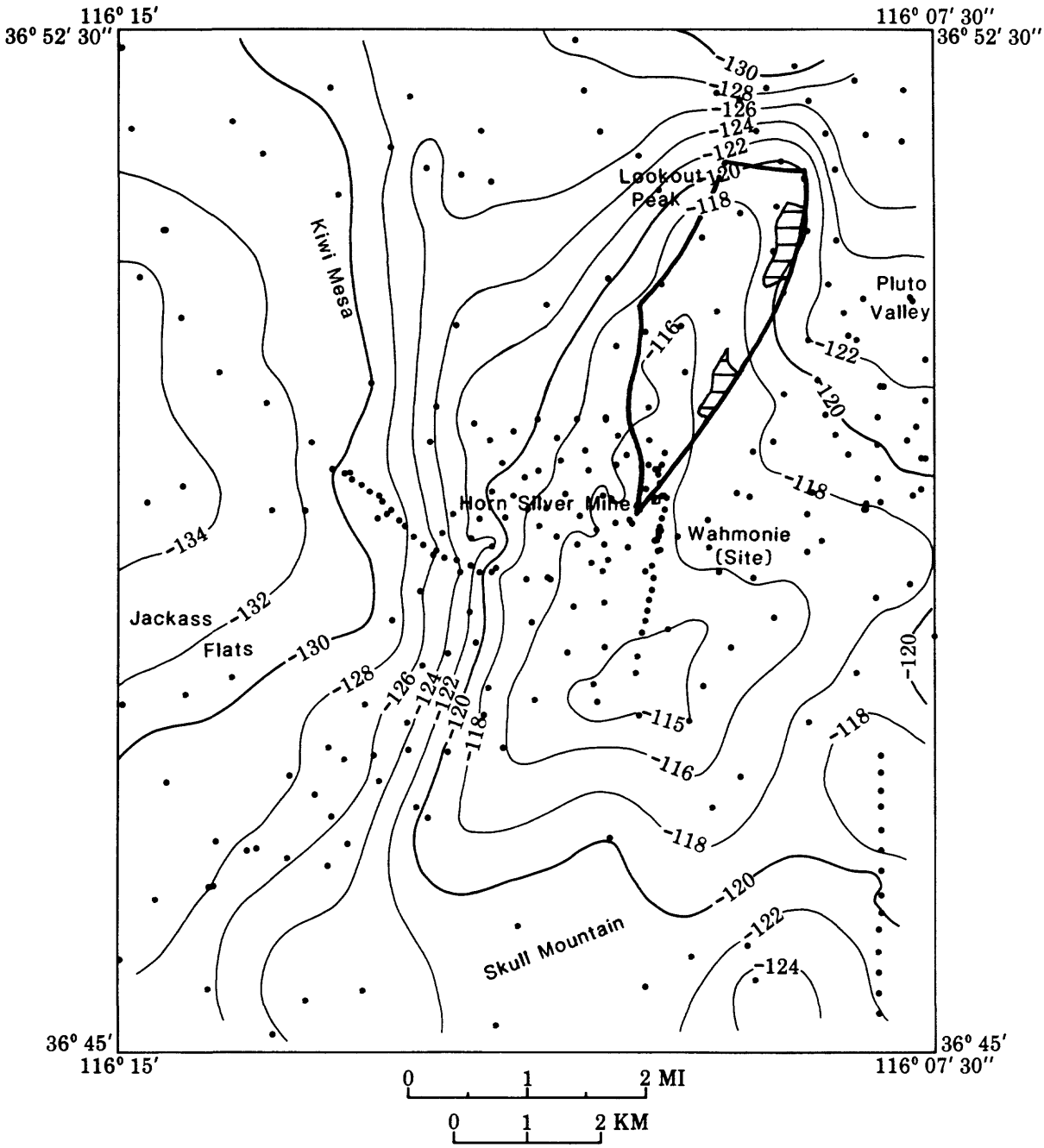

Figure 7.--Complete Bouguer anomaly contour map of the Skull Mountain 7½' quadrangle reduced for a density of 2.30 g/cm^3. The contour interval is 2 mGal. The Wahmonie horst is outlined. Granodiorite exposures are shown as ruled areas.

the Wahmonie horst, where the 2.30 g/cm^3 reduction density produces a sharper maximum over higher density rocks (2.55 g/cm^3). The Bouguer gravity anomaly located near Wahmonie Site does not appear to be dependent on topography but is clearly the expression of a dense body buried beneath the alluvium.

Residual Gravity

Plate 1 is the residual gravity anomaly map of the Skull Mountain 7½ minute quadrangle, reduced for a density of 2.67 g/cm^3, at a scale of 1:24,000, and at a contour interval of 1 mGal. A residual gravity anomaly map of the study area (ruled border area) and the surrounding vicinity reduced for a density of 2.67 g/cm^3 is shown in figure 8. Residual gravity values were computer calculated by removing a planar regional gravity gradient from the complete Bouguer anomaly values. The regional gradient was determined from Diment's (1961, fig. 2) regional gravity map of southern Nevada, which is based predominantly on data from gravity stations on pre-Tertiary rocks. Diment's map reflects density contrasts solely within the basement rocks and excludes anomalies caused by near-surface low-density rocks. Residual gravity anomaly values range from a minimum of -26 mGal to a maximum of -8 mGal on the Skull Mountain quadrangle and range to -7 mGal on the adjacent Cane Spring quadrangle. A datum shift of about -2.6 mGals exists between Diment's map and the Bouguer gravity anomaly values reported for Wahmonie Site.

The gravity data outline a large, broad, and flat-topped 15-mGal gravity high near Wahmonie Site. The maximum observed residual gravity anomaly value is -8.75 mGal at station W4S1 located about 610 m (2,000 ft) west of Wahmonie Site and about 610 m (2,000 ft) south of the Horn Silver mine. The steep gradient surrounding the high marks the boundaries of a structural high possibly associated with a felsic intrusive. The west and north edges of the high have an 8 mGal/km (12 mGal/mi) gravity gradient, while to the south a 6 mGal/km (9 mGal/mi) gradient exists between the high and the foot of Skull Mountain. At reduction densities of 2.50 and 2.30 g/cm^3 (figs. 9, 10), the decrease of the southern gradient to about 2 mGal/km (3 mGal/mi) indicates that the low density rocks of Skull Mountain are the source of much of the anomalous southern gradient. The linear north-trending gradient along the west edge of the high (fig. 8) represents a steeply dipping contact at depth which suggests the presence of a fault. This interpretation of the buried contact is supported by electrical resistivity data where a fault has been interpreted at about 2.9 km (1.8 mi) west of Wahmonie Site with the west section downdropped (Christian Smith and others, written commun., 1979).

The gravity field rapidly decreases west of the anomalous high to a broad, flat closed low of the -24 mGal contour over Jackass Flats (fig.

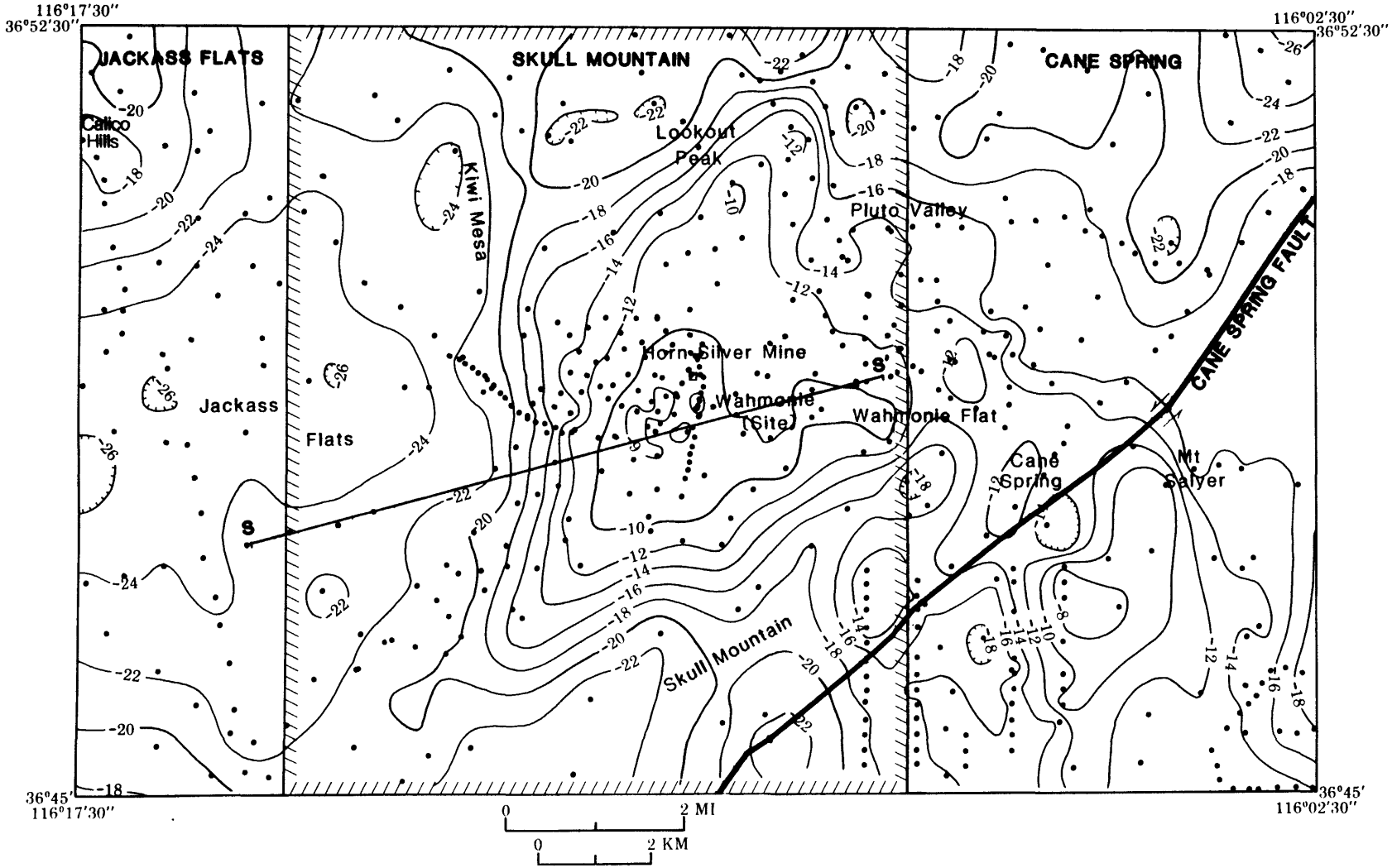

Figure 8.--Residual gravity anomaly contour map of the Skull Mountain and part of the Jackass Flats and Cane Spring 7½' quadrangles reduced for a density of 2.67 g/cm^3. The contour interval is 2 mGal. Hachures indicate closed gravity lows. Ruled border area is shown in plate 1.

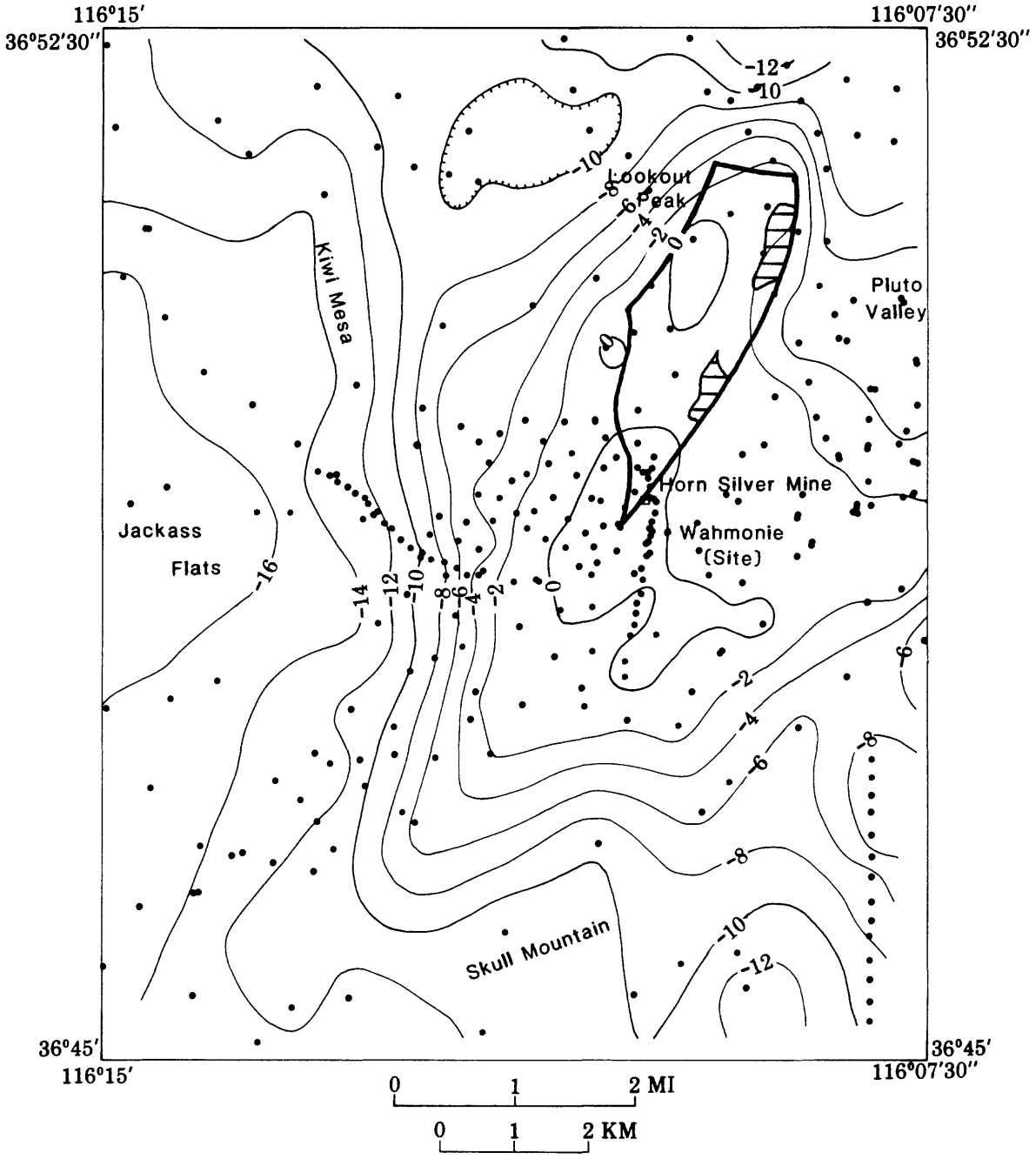

Figure 9.--Residual gravity anomaly contour map of the Skull Mountain 7½' quadrangle reduced for a density of 2.50 g/cm^3. The contour interval is 2 mGal. The Wahmonie horst is outlined. Granodiorite exposures are shown as ruled areas. Hachures indicate closed gravity lows.

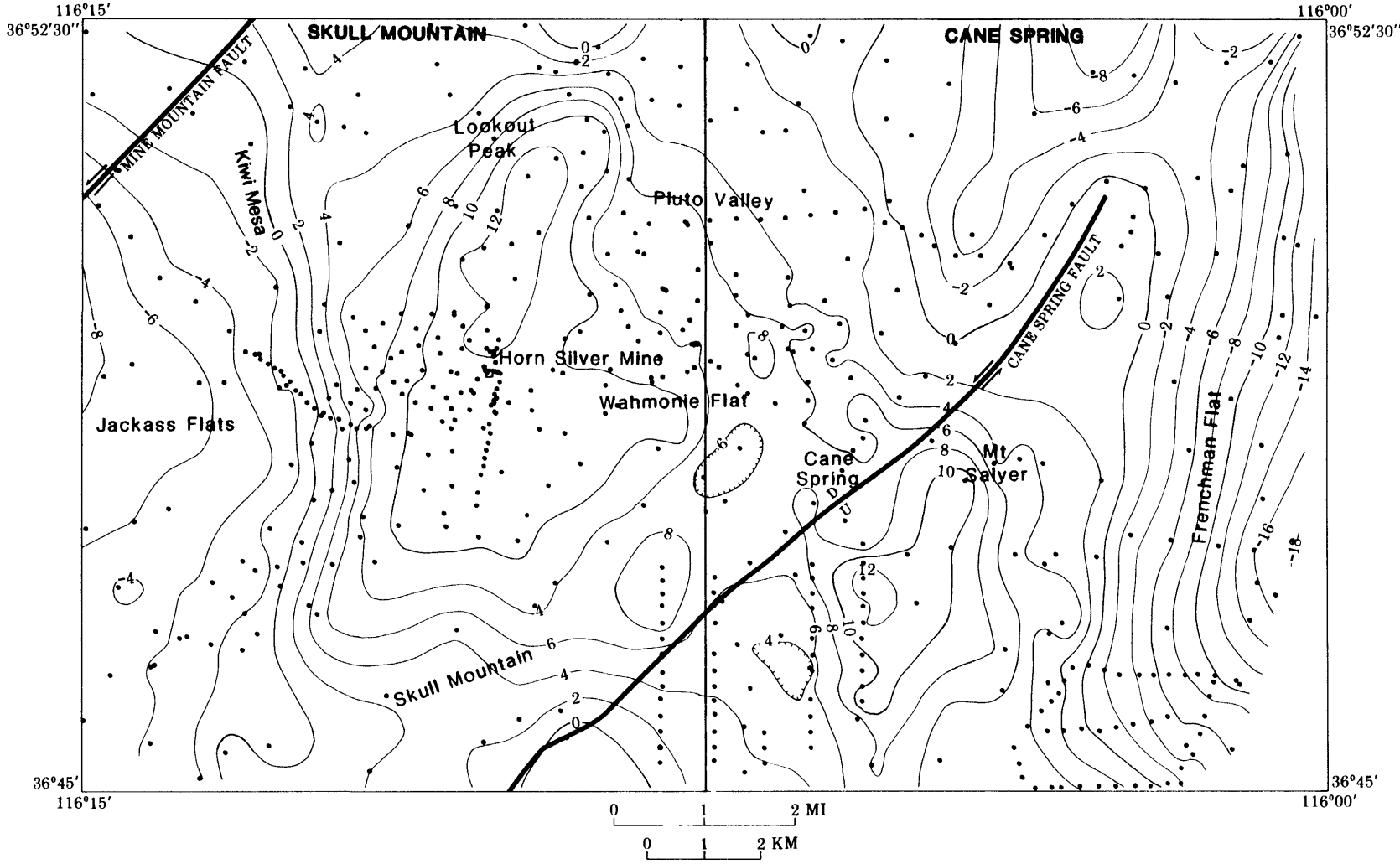

Figure 10.--Residual gravity anomaly map of the Skull Mountain and Cane Spring 7½' quadrangles reduced for a density of 2.30 g/cm^3. The contour interval is 2 mGal. Hachures indicate closed gravity lows.

8). This decrease partly reflects an increase in alluvial thickness to 150 m (500 ft) at well J-11, in Jackass Flats (table 2). The east edge of the anomalous high extends southeast, where the gravity field becomes much more irregular (fig. 8). This area is further obscured by a linear series of local highs and lows that follows the general NNE. trend of the left-lateral Cane Spring fault. Its change in strike from north to northeast is caused in part by drag and rotary slippage along the right-lateral Las Vegas Valley shear zone to the south of the study area (Ekren, 1968, p. 16-17). Farther east a linear set of contours with a gradient of about 4 mGal/km (6 mGal/mi) parallels Frenchman Flat (fig. 10).

The three-dimensional expression of the residual gravity anomaly field of the Skull Mountain quadrangle reduced for a density of 2.67 g/cm^3 is shown in figure 11. The portrayal is equivalent to viewing plate 1 from the SW. corner of the map. The steep gradients, particularly the gradient on the west side of the anomaly, are clearly visible.

South-North Gravity Profile

The south-north regional gravity anomaly profile along line 1A-1D (fig. 12, plate 1) shows the relation between gravity, aeromagnetics, and topography. The residual gravity anomaly profile shows the steep gradient of 6 mGal/km (9 mGal/mi) at the edge of the anomaly and the broad relatively flat high. Aeromagnetic data correlate well with the gravity data. The magnetic maximum is slightly offset to the south of the gravity high, suggesting that the causative body is normally magnetized. The sharp magnetic spike at the northern foot of Skull Mountain is caused by edge effects at the termination of the anomaly-producing rocks of Skull Mountain. Although the gravity low over Skull Mountain is partially produced by a too-high reduction density (2.67 g/cm^3), gravity stations south of Skull Mountain indicate that the "low" is the background level for the anomalous high centered near Wahmonie Site. The anomalous gravity maximum from 1B-1C of figure 12 is shown in more detail on figure 13. The segment of the profile from 1B-1C is coincident with a ground magnetic survey by G. D. Bath (written commun., 1980). The gravity and magnetic profiles show excellent correlation with one another and no correlation with the topographic low along Cane Spring Road. The small gravity peak of about 1 mGal may represent a cupola (an offshoot from the main mass), or a local structural high in the basement rocks. Using Nettleton's (1940, p. 12) half-width method of approximating the depth to center of mass of the cupola, modeled as a horizontal cylinder, yields an estimate of about 110 m (400 ft). Magnetic data indicate that the depth to the top of the cupola using the maximum horizontal extent of the steepest gradient (Vacquier and others, 1951, p. 12) is less than about 50 m (160 ft) assuming a prismatic model. Electrical resistivity data within the zone of hydrothermal

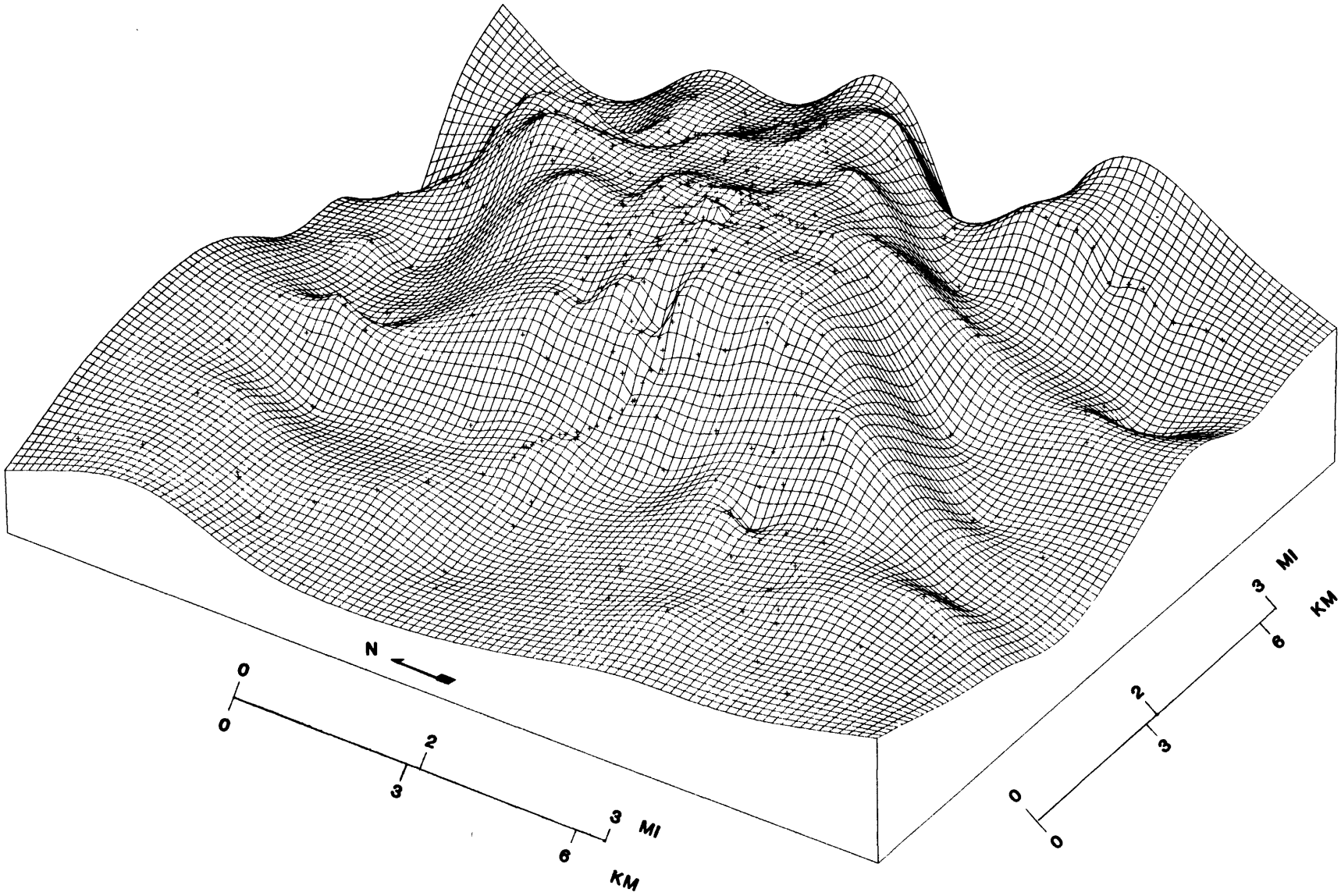

Figure 11.--Three-dimensional mesh perspective view of the residual gravity anomaly field of the Skull Mountain 7½' quadrangle reduced for a density of 2.67 g/cm^3. The view angle is from the SW. corner of plate 1. Gravity stations are plotted at their correct spatial positions.

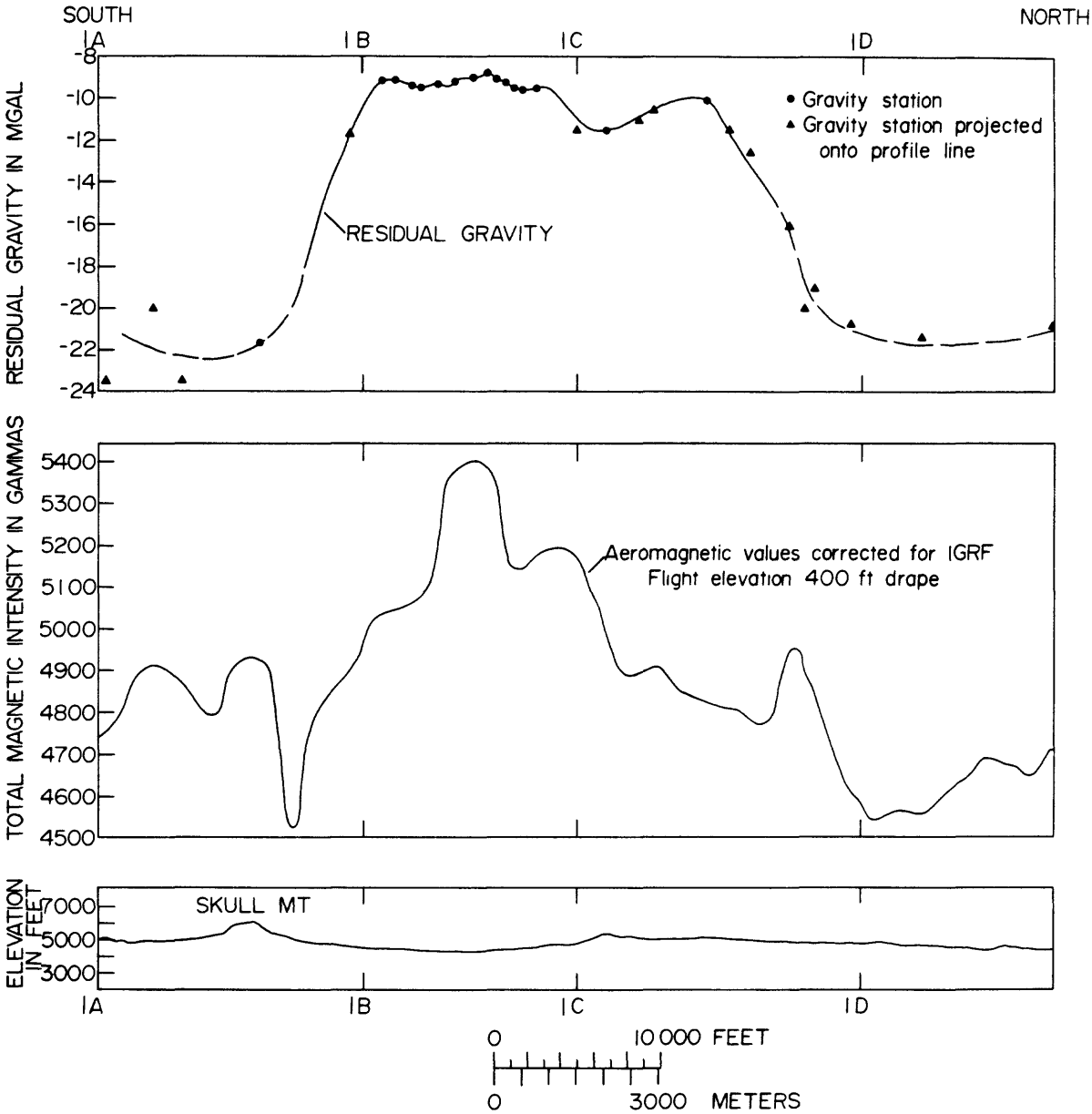

Figure 12.--South-north residual gravity anomaly profile line 1 reduced for a density of 2.67 g/cm^3. The profile is located on plate 1. Residual aeromagnetic values are corrected for IGRF 1975 with a 5,000-gammma constant added. The detailed profile from 1B-1C is shown in figure 13.

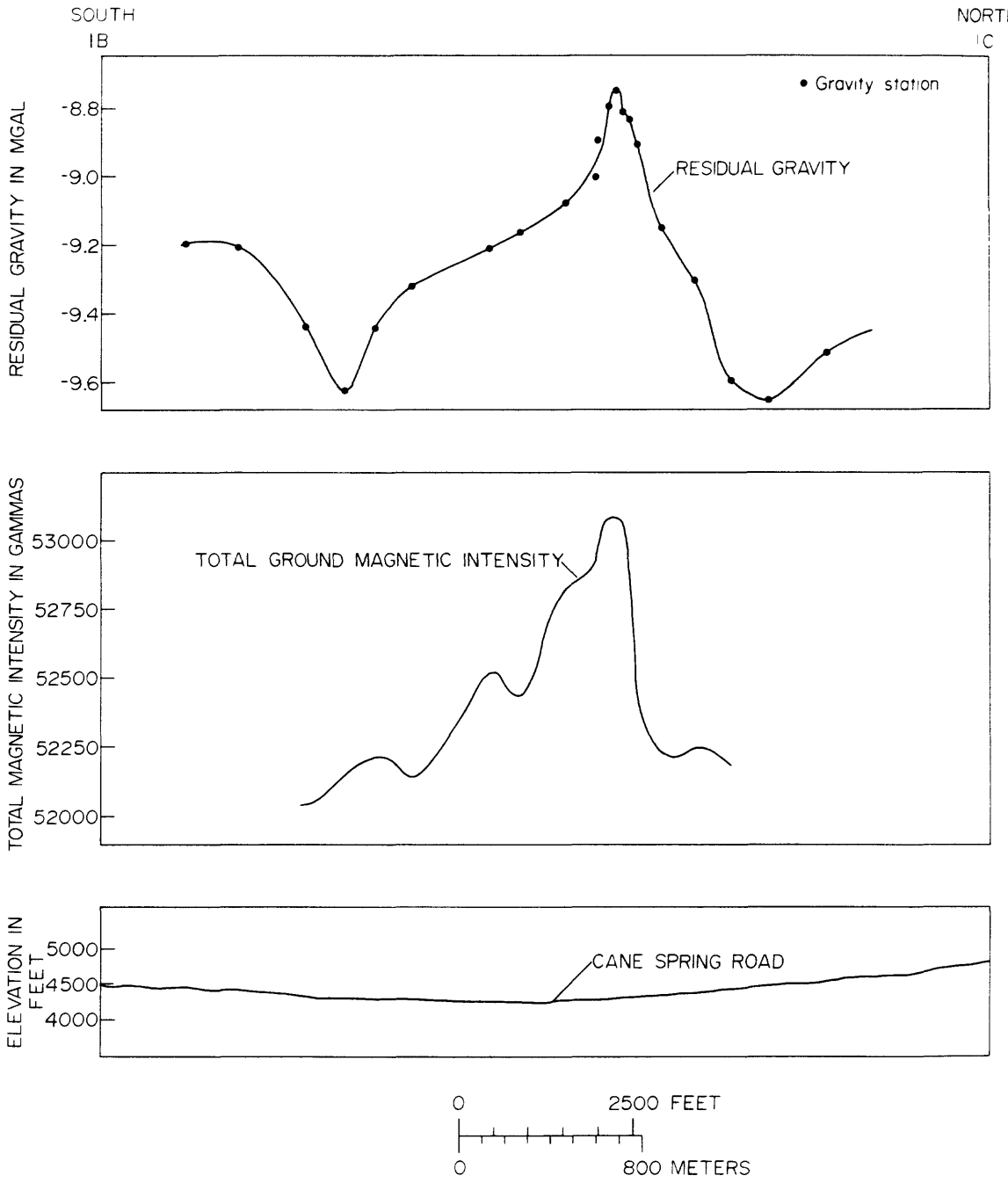

Figure 13.--Detailed south-north residual gravity profile line 1 coincident with a ground magnetic traverse. The profile is located on plate 1.

alteration near Wahmonie Site suggests that an intrusive body may be present where the resistivity begins to increase at a depth as shallow as 50 m (160 ft). The absence of a sharp resistive boundary here suggests that the inferred intrusive rocks, with the main body approximately 610 m (2,000 ft) below the surface near Wahmonie Site may be significantly altered (D. B. Hoover, written commun., 1980).

Gravity and Seismic Refraction Data Line 2

There are preliminary data from three seismic refraction lines across the Wahmonie Site area. Line SS', located along Cane Spring Road (fig. 8), is a fan shot with the shot point located about 60 km (37 mi) NNW. of Wahmonie Site (J. H. Healy, written commun., 1980). The relation between residual gravity and reduced seismic refraction travel time is shown in figure 14. Reduced seismic travel time was computed by subtracting X/6.0 from the one-way travel time (T), where X is the distance from shot point to detector in km, and 6.0 is the seismic velocity of a deep homogeneous medium in km/sec. Although the data are preliminary, the profile shows a decrease in reduced travel time that correlates with an increase in residual gravity. The decrease in travel times suggests that the causative body underlies the Wahmonie Site area. It is not likely that the high-velocity body is nearer the shot-point because as seismic ray paths converge closer to the shot-point more seismic records would display the anomalous times. Also, the seismic rays are deep throughout most of their paths, in a homogeneous medium of about 6.0 km/sec (20,000 ft/sec) (Diment and others, 1961, p. 212).

The second seismic refraction profile is along line 2B-2C (plate 1). A two dimensional model of the data (L. W. Pankratz, written commun., 1980) is shown in figure 15 along with a residual gravity anomaly profile. At least four seismic refraction groups can be identified which can be correlated with lithologic units in the area. Table 4 summarizes several probable correlations of seismic velocity to lithology. The first velocity group, of 1.0 to 2.2 km/sec (3,200 to 7,200 ft/sec), is typical of alluvial velocities. The second group ranges in velocity from 2.6 to 3.2 km/sec (8,500 to 10,000 ft/sec) and is believed to represent volcanic tuffs and hydrothermally altered rocks at Wahmonie Site.

Hypothesis 1 (table 4) considers the third velocity group to represent fractured granite or rhyodacite similar to that exposed in the Wahmonie horst. However, the small range in seismic velocities in the third velocity group suggests that this layer is not significantly fractured, reducing the likelihood for the occurrence of fractured granite or rhyodacite (L. W. Pankratz, oral commun., 1980).

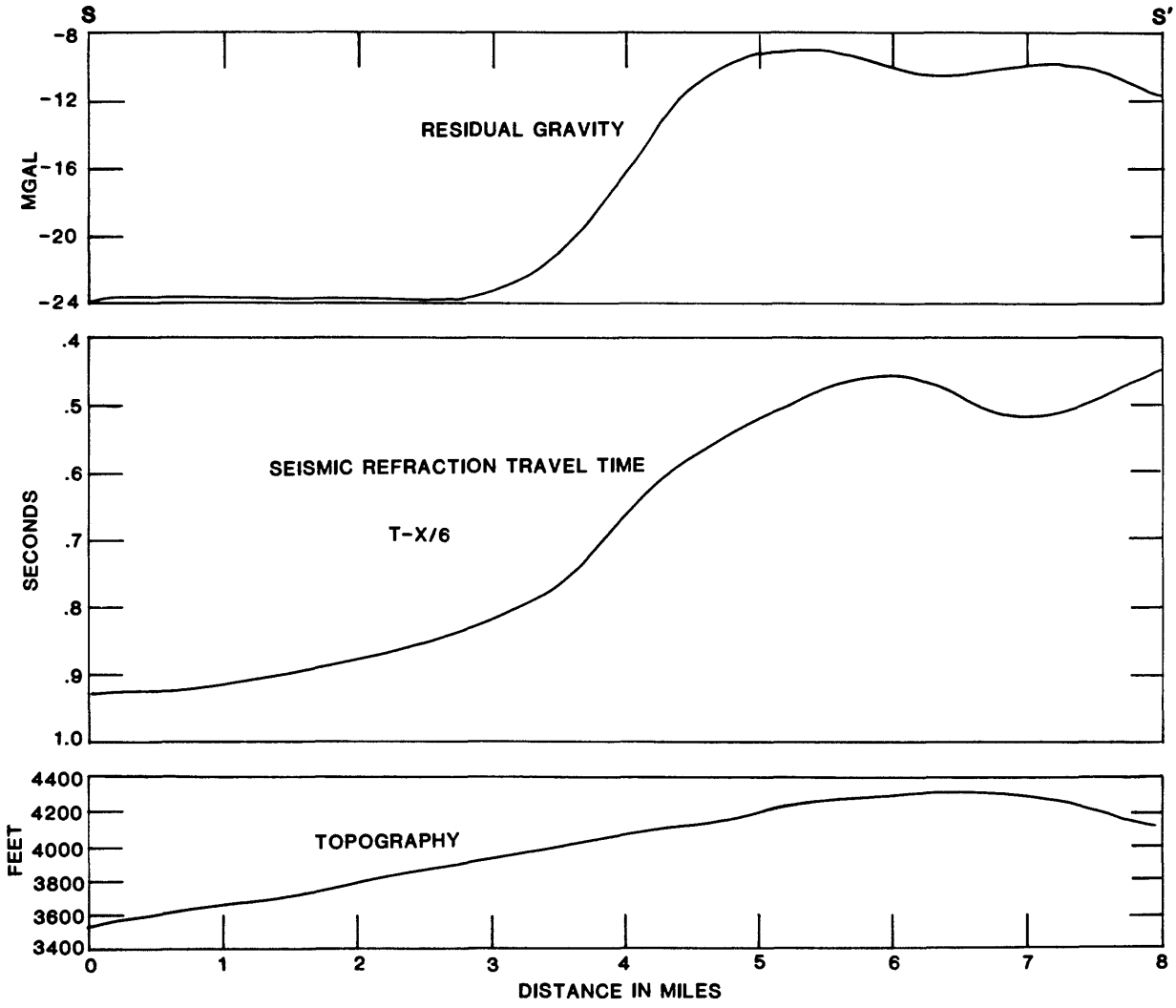

Figure 14.--Seismic profile along Cane Spring Road shows correlation of reduced seismic travel times and residual gravity anomaly reduced for a density of 2.67 g/cm^3. The profile line SS' is located on figure 8.

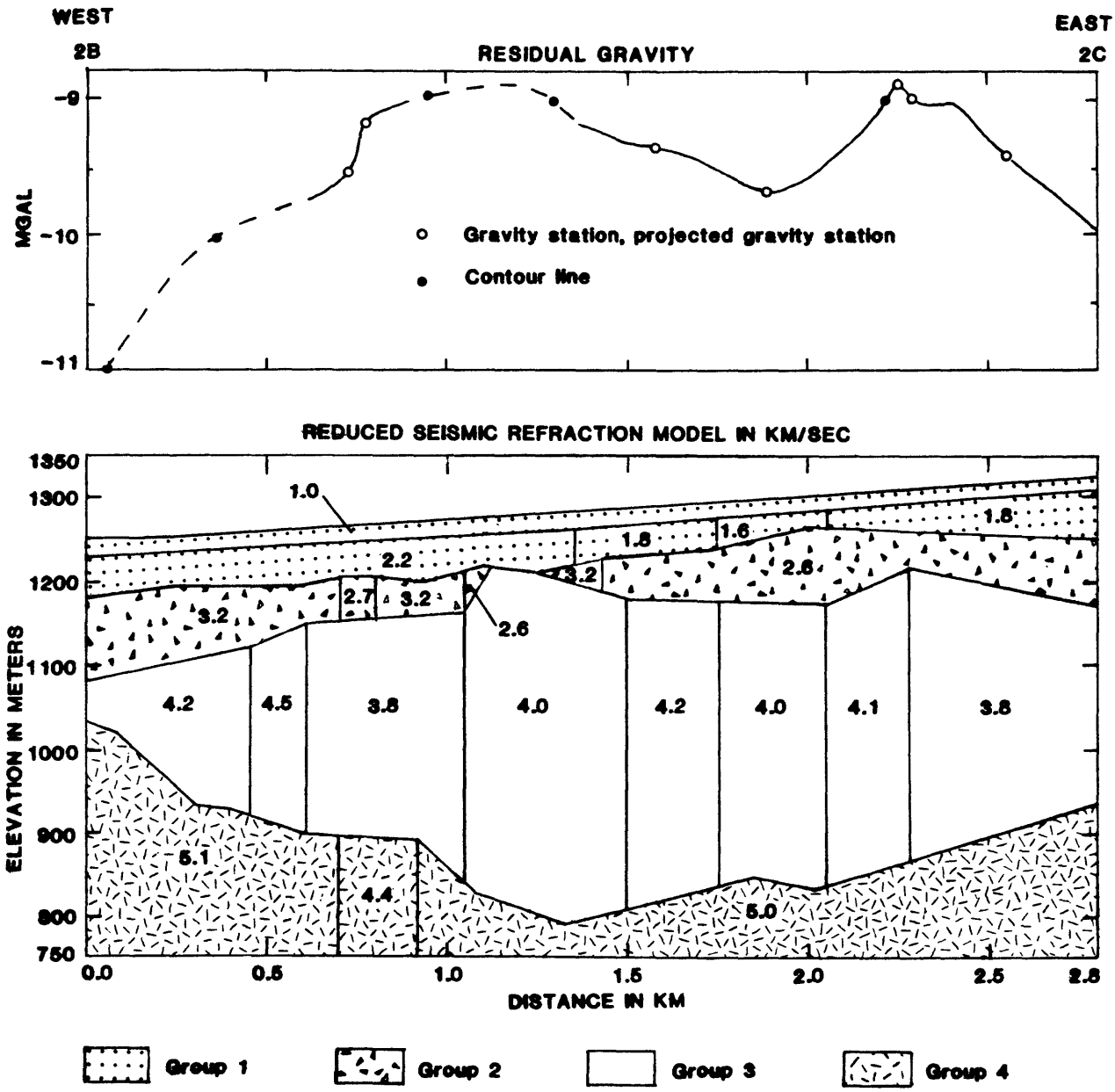

Figure 15.--Seismic refraction model along profile 2 by L. W. Pankratz (written commun., 1980) and residual gravity anomaly reduced for a density of 2.67 g/cm^3. The profile is located on plate 1.

Table 4.--Correlation of seismic velocity group to lithology

Velocity group	Range of velocity (km/sec)	Range of density (g/cm^3)	Hypothesis 1	Hypothesis 2	Hypothesis 3
1	1.0-2.2	1.90	Alluvium	Alluvium	Alluvium
2	2.6-3.2	2.00-2.35	Tuff	Tuff	Tuff
3	3.8-4.5	2.40-2.55	Fractured granite or rhyodacite.	Altered argillite.	Altered argillite.
4	4.4-5.1	2.65-2.67	Granite	Marble	Granite

In the Calico Hills area, a surface Vibroseis survey with a geophone that recorded downhole signals reported average interval velocities in drill hole UE25a-3 (fig. 2) for an upper argillite at 2.0 km/sec (6,600 ft/sec), a lower argillite at 3.2 km/sec (10,000 ft/sec), an altered argillite at 4.1 km/sec (13,000 ft/sec), and a marble at 5.1 km/sec (17,000 ft/sec) (Maldonado and others, 1979, p. 41). These seismic velocities suggest an alternate hypothesis in which the third and fourth velocity groups at Wahmonie Site might represent altered argillite and marble of the Eleana Formation (hypothesis 2, table 4). However, the difference in geology at Calico Hills and Wahmonie Site and the requirement that the causative body is strongly magnetic, reduce the likelihood of the occurrence of marble as a source of the gravity and magnetic highs.

The third hypothesis (table 4) suggests that the third velocity group represents altered argillite. The velocity group correlates well with the seismic velocities recorded for the altered argillite layer at Calico Hills. Moreover, electrical resistivity studies suggest that a member of the Eleana Formation might underlie the Wahmonie Site area (D. B. Hoover, written commun., 1980). The fourth seismic velocity group has a velocity of about 5.0 km/sec (16,000 ft/sec) and probably represents granitic rocks similar to and possibly contiguous with the granodiorite outcrops of the Wahmonie horst.

The two structural highs in the third velocity group correlate well with two gravity maxima at 1.2 km (.75 mi) and 2.3 km (1.4 mi) east of point 2B in figure 15. Two-dimensional gravity modeling along the seismic traverse (fig. 20) shows that the density distribution equivalent to the velocity group distribution reproduces the eastern gravity gradient and the necessary amplitude of the gravity maximum. A

sharp lateral change in density, probably due to a vertical fault, must be placed at about -0.4 km (-0.2 mi) from point 2B to produce the observed western gradient. This lateral change in density coincides with the location of the outer edge of the zone of hydrothermal alteration on the geologic map by Ekren and Sargent (1965). Magnetic data at the NTS suggest that the Eleana Formation has no members with significant magnetizations. However, at Calico Hills, about 15 km (9.3 mi) NW. of Wahmonie Site (fig. 2), an altered facies of the Eleana Formation is locally magnetic (Snyder and Oliver, 1981, p. 11). It is difficult to ascertain if an altered argillite underlies the magnetic high near the Wahmonie Site. If locally magnetic argillite does occur beneath Wahmonie Site, its lateral extent would be very limited in an east-west direction because the magnetic anomaly has a marked northward trend. Further reducing the likelihood that an underlying member of the Eleana Formation causes the magnetic high is the close association of local magnetic highs with granodiorite exposures north of the Horn Silver mine (figs. 4, 5).

Gravity and Seismic Refraction Data Line 4

Residual gravity reduced for a density of 2.67 g/cm^3, aeromagnetic data, and topography with generalized geologic surface outcrops for line 4A-4D (plate 1) are shown in figure 16. A local gravity high of about 1.7 mGal is centered directly over the southern granodiorite exposure. The horizontal extent of the high suggests that the granodiorite body is broader than it's surface expression, about 1.0 km (0.62 mi). The gravity high is located at the east edge of the Wahmonie horst and is related to the granodiorite body. A finite sheet approximation with a width of 1.0 km (0.62 mi) and depth to top of body of 0.20 km (0.12 mi) suggests that the body extends to a depth of about 1.0 km (0.62 mi). An aeromagnetic anomaly correlates with the gravity high and is much more narrow suggesting that the granodiorite body may have a central core of high susceptibility material or that the broader gravity high may be closer associated with the horst structure than with the granodiorite outcrop. The later may be possible because the observed density contrast between the horst, composed predominantly of rhyodacite, and the granodiorite is only 0.06 g/cm^3. Clearly, the small pip on the gravity profile with an amplitude of 0.30 mGal, which directly overlies the granodiorite outcrop is caused by the granodiorite.

A third seismic refraction profile is along line 4B-4C (plate 1). A two-dimensional model of the data (L. W. Pankratz, written commun., 1981) indicate there are approximately five seismic layers (fig. 17). The three uppermost layers have velocities typical of alluvium ranging to 1.28 km/sec (4,200 ft/sec). The fourth layer ranges in velocity from 3.2 to 4.8 km/sec (10,000 to 16,000 ft/sec) and has an anomalous low velocity zone of 2.3 km/sec (7,500 ft/sec) from a distance of about 550 to 900 m (1,800 to 3,000 ft) that extends into layer five. The fifth

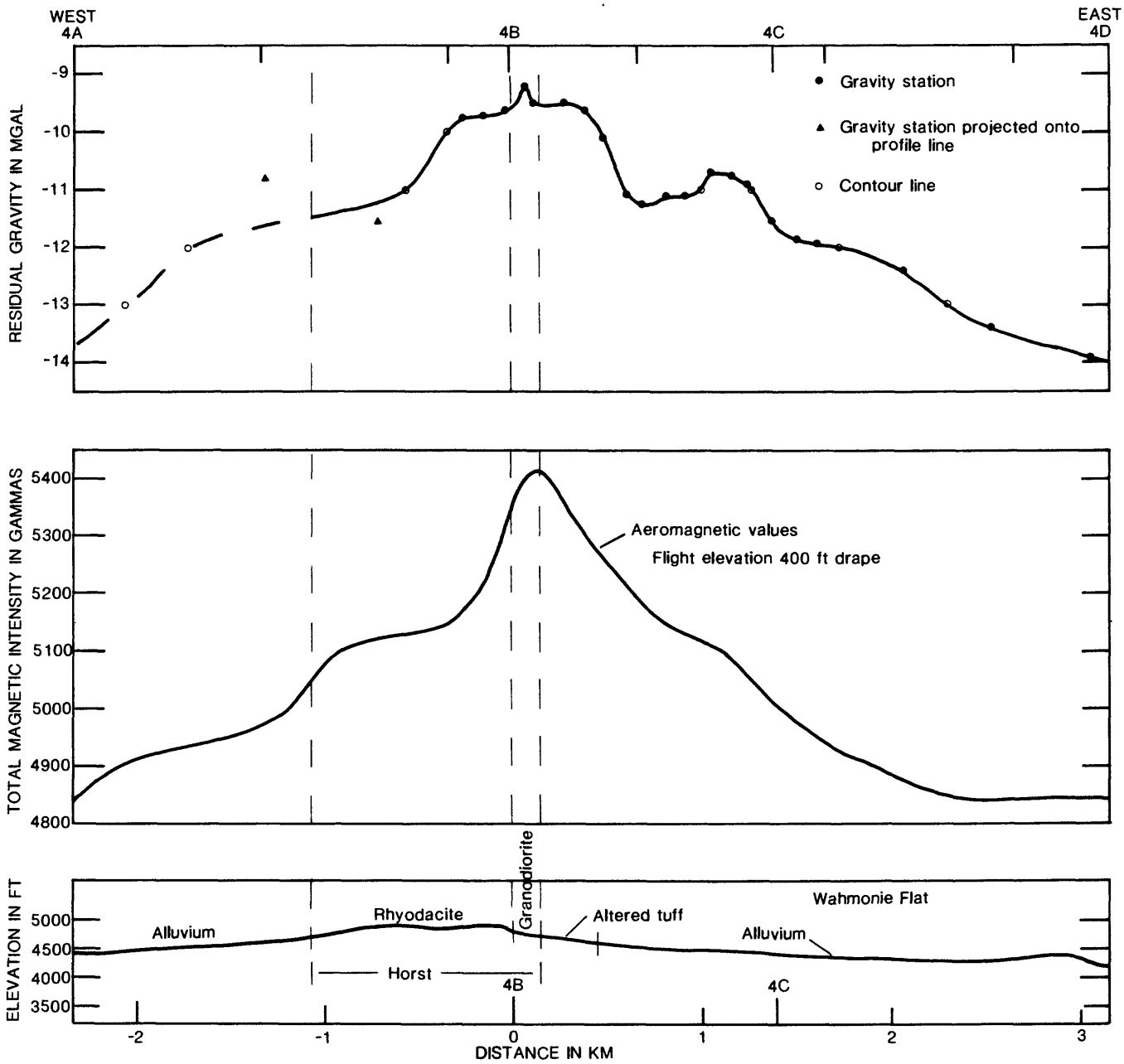

Figure 16.--Residual gravity anomaly profile line 4 reduced for a density of 2.67 g/cm^3. The profile is located on plate 1. Residual aeromagnetic values are corrected for IGRF 1975 with a 5,000-gamma constant added. The detailed profile from 4B-4C is shown in figure 17.

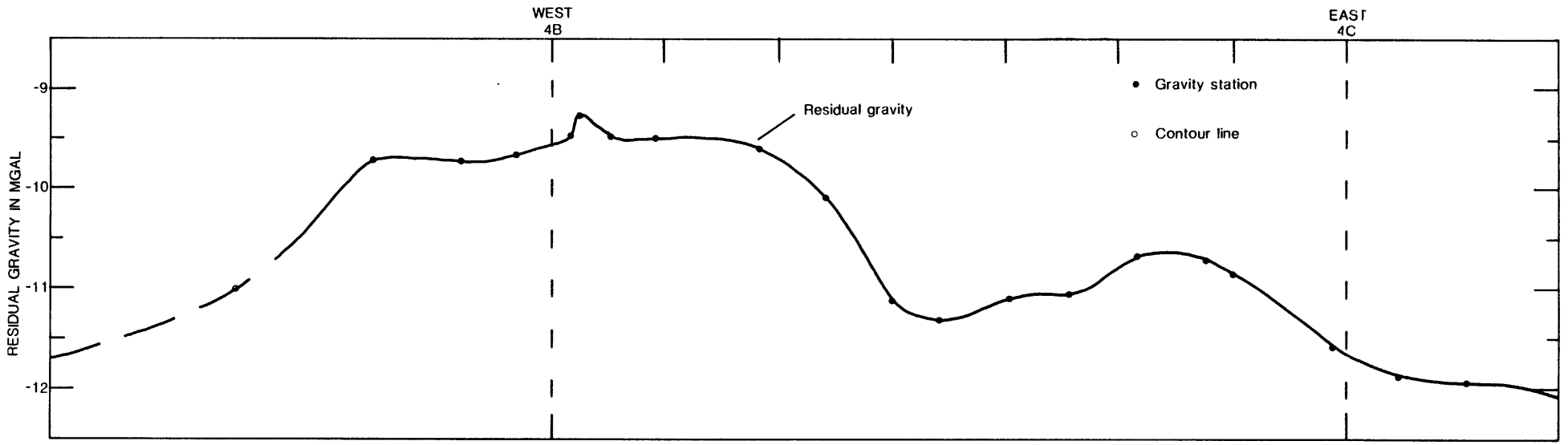

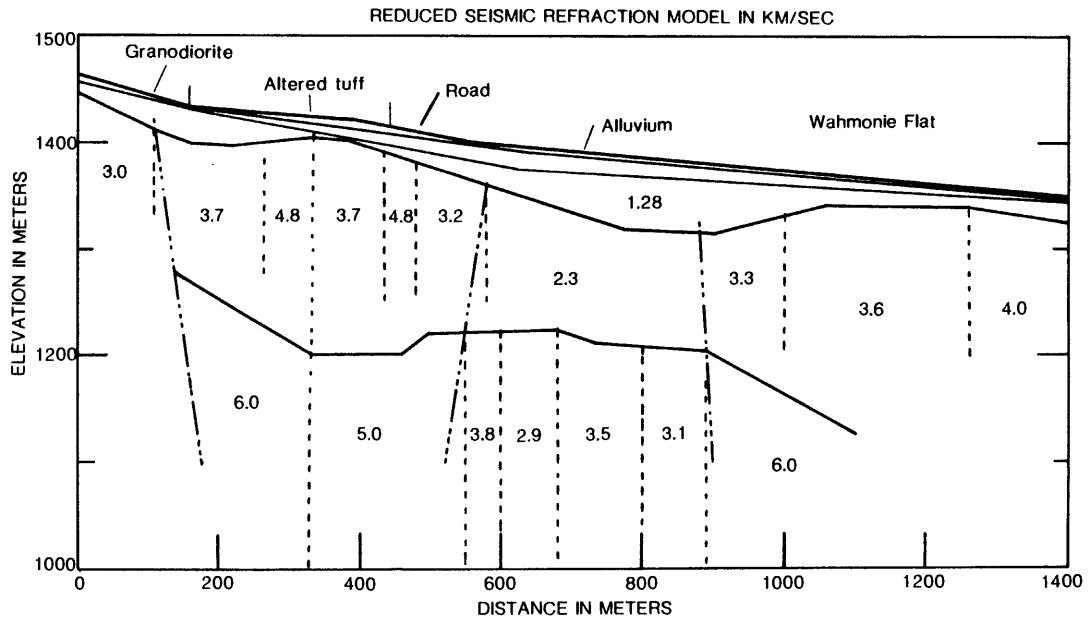

Figure 17.--Seismic refraction model along profile line 4 by L. W. Pankratz (written commun., 1981) and residual gravity anomaly for a density of 2.67 g/cm^3. The profile is located on plate 1.

layer has velocities consistent with values for granitic rocks of about 5.0 to 6.0 km/sec (16,000 to 20,000 ft/sec). The seismic model which supports the gravity data shows that the granitic body extends eastward to a distance of 550 m (1,800 ft). The model shows that the main part of the granitic body is about 200 m (700) below the surface.

The low velocity zone from 550 to 900 m (1,800 to 3,000 ft) correlates to a decrease in the residual gravity field which then increases eastward to a local gravity high at a distance of 1.1 km (0.68 mi). The horizontal extent of the maximum gradient indicates that the high at 1.1 km (0.68 mi) is caused by a body at a depth of about 200 m (700 ft), which correlates with a 6.0 km/sec (20,000 ft/sec) seismic velocity layer (fig. 17)

GRAVITY MODELING

Problems of Interpretation

Gravity interpretations based on gravity data alone do not produce unique solutions. This arises from the fact that a given gravity distribution can be produced by an infinite number of mass or density distributions. Because of the inherent ambiguity of the method, other control is necessary to discriminate between possible solutions.

Geologic information is not available below an elevation of 1,100 m (3,600 ft) in the area of the anomalous gravity and magnetic highs at Wahmonie Site. Drill holes in eastern Wahmonie Flat give no clue to subsurface structure or lithology because they were located predominantly in dacite porphyry of the Wahmonie Formation. (See Johnson and Ege, 1964, p. 93-126.) However, several independent geophysical methods provide some of the depth and lithologic control necessary to evaluate the gravity data. Seismic methods near Wahmonie Site yield seismic velocities and density-velocity interfaces that may be approximated to lithologic units. Electrical methods provide information on resistivity layers that can be correlated to rock units in nearby wells and drill holes. Magnetic data furnish depth estimates and show that the causative body is strongly magnetic.

Methods

Gravity modeling of each profile involved the use of an updated revision of Talwani and others (1959, p. 49-59) two-dimensional gravity modeling program (H. W. Oliver, written commun., 1980). The program utilizes polygons to approximate the shape of bodies with various

density contrasts and computes the vertical component of their gravitational attraction. The computations are tedious but are readily computer programmable. A functional operating procedure is to estimate mass distribution based on all available information, calculate the gravity effect, compare the calculated and observed gravity anomalies, and then modify the mass distribution within the limits set by the independent control until a satisfactory fit is achieved. The procedure is facilitated by the use of two- and three-dimensional modeling techniques described by Talwani and others (1959), Talwani and Ewing (1960), Tanner (1967), Cordell and Henderson (1968), and Cady (1980).

South-North Gravity Model Line 1

The south-north residual gravity anomaly profile shown in figures 12 and 13 was interpreted with the resulting model shown in figure 18. The profile line 1A-1D strikes N.10°E., begins at Skull Mountain, continues across the low drainage divide betwen Jackass Flats and Wahmonie Flat, traverses the Wahmonie horst, and ends NE. of Lookout Peak (plate 1). The profile from 1B-1C has gravity stations spaced at 100 m (328 ft) intervals and coincides with a ground magnetic traverse (fig. 12). The model is based on geologic and magnetic data. Density contrasts were based on bulk density samples listed in table 3 and were subsequently modified to achieve a better fit between calculated and observed residual gravity.

The model includes the low-density volcanic rocks of Skull Mountain (2.00 to 2.15 g/cm$^{3)}$ with an inferred basement at about sea level, 1.4 to 1.6 km (4,600 to 5,200 ft) below the ground surface. A thick sequence of low-density material is required to produce the low observed gravity values at Skull Mountain. The presence of this layer is partially substantiated by geologic data that show the tuffaceous rocks of eastern Skull Mountain extending to an elevation of about 980 m (3,200 ft), below which the stratigraphy and structure is unknown (Poole and others, 1965). The geology represented by the model is shown schematically in figure 19.

Low-density (1.90 g/cm^3) alluvial deposits are at the surface of Wahmonie Flat (plate 1). Seismic refraction results indicate that the thickness of alluvium ranges from about 30 to 70 m (100 to 230 ft) near Wahmonie Site. Moderately dense rocks (2.50 g/cm^3) beneath the alluvium may represent highly fractured or altered granitic rocks, rhyodacite, or argillite of the Eleana Formation. There is no direct geologic evidence to support the occurrence of the Eleana Formation beneath the Wahmonie Site. However, electrical studies in the area show resistivities that are consistent with values reported for an argillite member of the Eleana Formation. A body with a density of 2.67 g/cm^3 is inferred to intrude the 2.50 g/cm^3 rocks and includes offshoots from the main mass to achieve a better agreement between calculated and observed gravity anomalies.

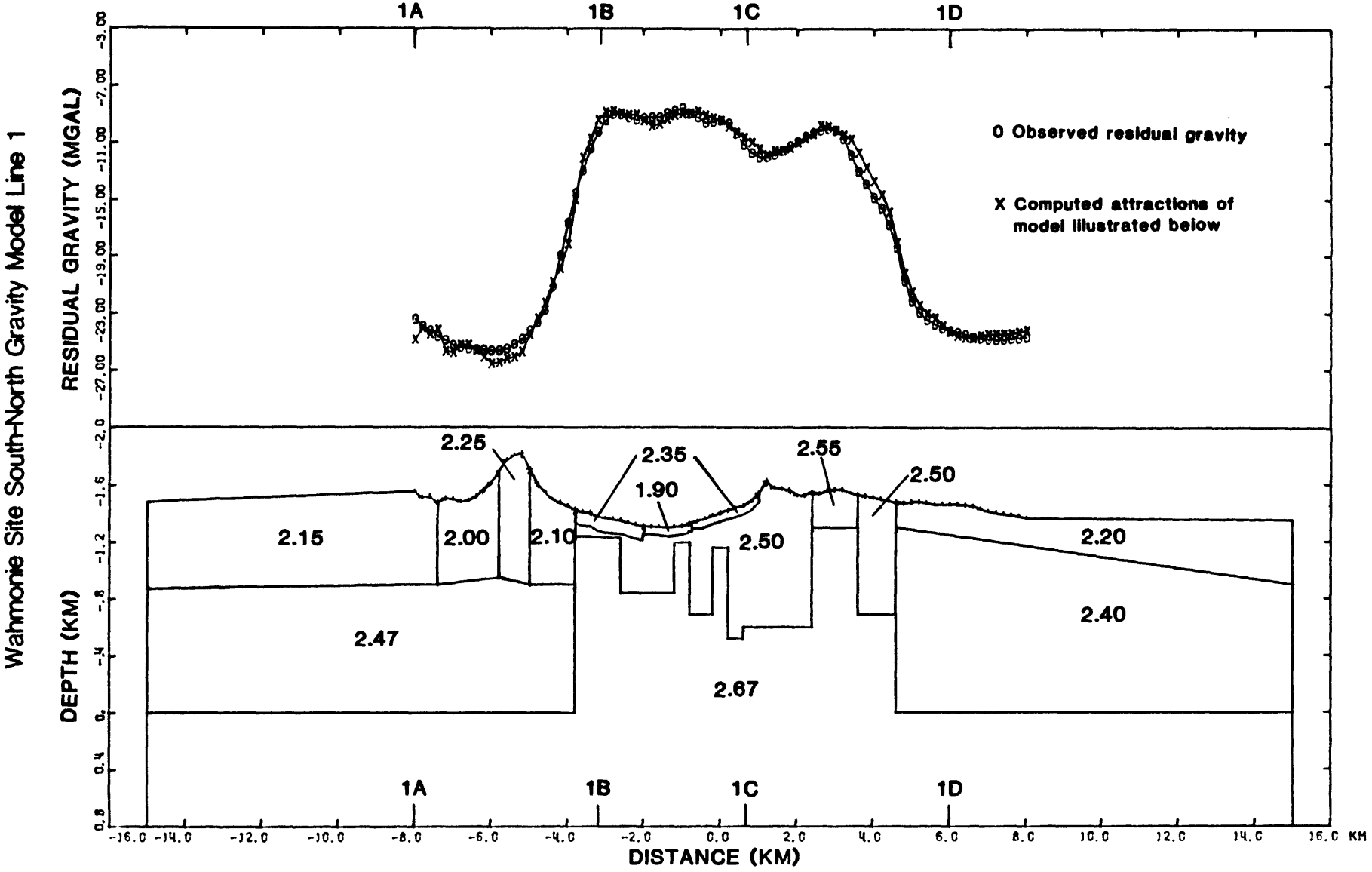

Figure 18.--South-north residual gravity interpretive model line 1. Densities (g/cm^3) are based on rock sampling. The profile is located on plate 1. A schematic of the geology is shown in figure 19.

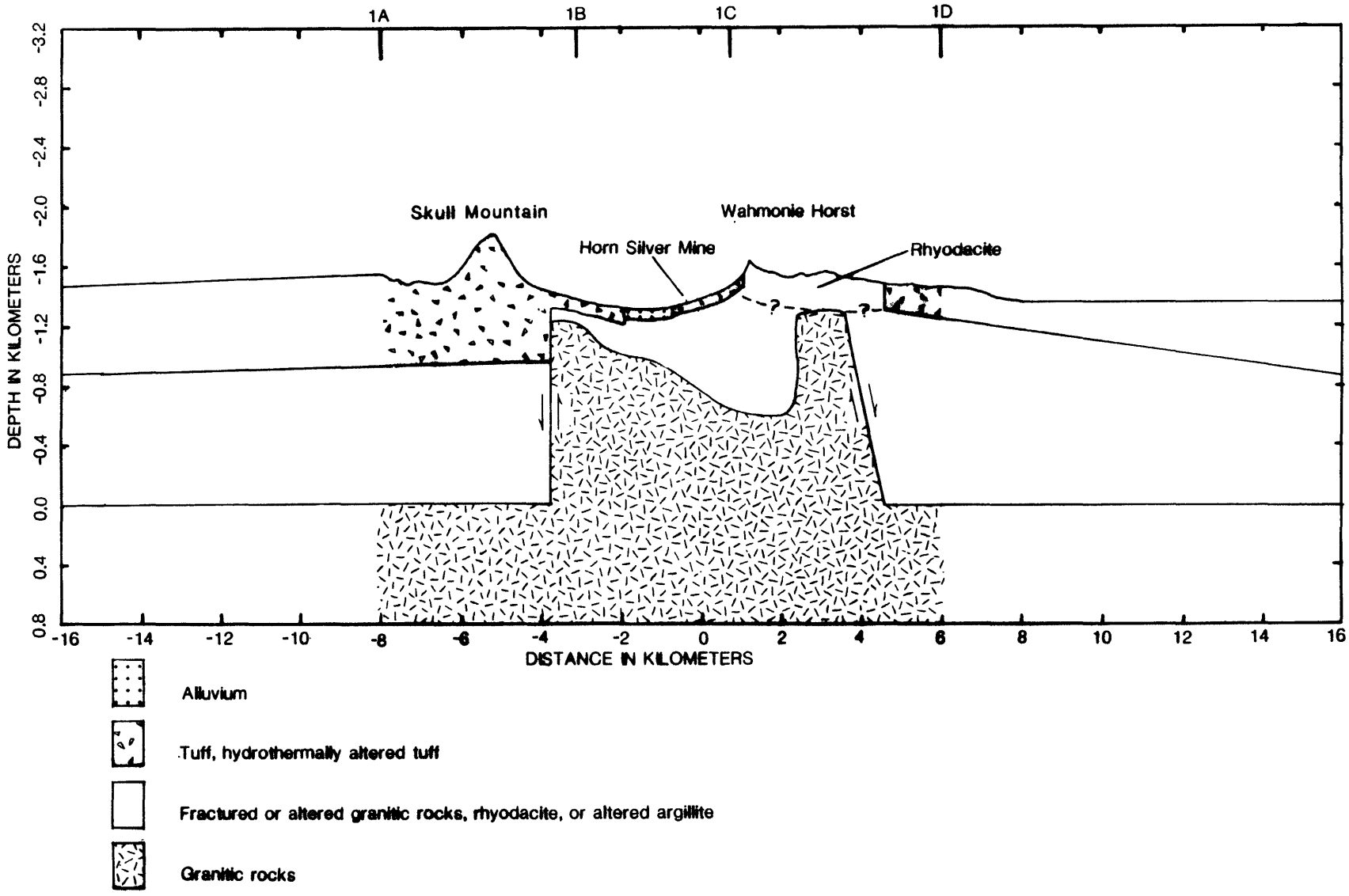

Figure 19.--Schematic of the geology represented in model line 1, figure 18.

Rocks of the Wahmonmie horst are relatively dense. Eleven samples of rhyodacite from the Salyer Formation average 2.59 g/cm^3 (table 3). A dense 2.67 g/cm^3 body is also shown in figure 18 to extend beneath the horst. It's presence is supported by the geologic cross-section of Ekren and Sargent (1965). North of the horst, exposed lower density tuffaceous rocks are shown collectively as a 2.20 g/cm^3 body. The steep gravity gradients along the edges of the maximum are produced by a near-vertical contact or fault with a moderate density contrast of 0.30 g/cm^3.

Although the south-north profile assumes intrusive rocks beneath Wahmonie Site, it correlates well with the geologic and physical properties of the area. The main mass of the causative body is shown at a depth of about 610 m (2,000 ft).

Gravity-Seismic Model Line 2

The model shown in figure 20 is based on the seismic refraction model shown in figure 15. Other parts of the gravity model have been extrapolated from this section. The profile line 2A-2D begins in western Wahmonie Flat, strikes N.68°E., and ends in eastern Pluto Valley on the Cane Spring quadrangle. The seismic refraction model (fig. 15) provides control for a distance of 0.0 to 2.8 km (0.0 to 1.7 mi) and to an elevation of 750 m (2,460 ft).

The four seismic velocity groups indicated in figure 15 and discussed above may be assigned density values based on velocity and inferred lithology (table 4). The first group which has seismic velocities typical of alluvium is assigned a density of 1.90 g/cm^3. The second velocity group, believed to represent hydrothermally altered volcanic tuffs, is assigned a density of 2.35 g/cm^3 on the basis of rock sampling in Wahmonie Flat. The third velocity group, which has seismic velocities similar to those reported for altered argillite at Calico Hills, is assigned a density of 2.55 g/cm^3 on the basis of drill-core samples from Calico Hills and rhyodacite samples from the Wahmonie horst. The fourth group is assigned a density of 2.65 g/cm^3 on the basis of 23 samples of granodiorite from the Wahmonie horst. These velocity to density conversions are consistent with the general empirical values of Woolard (1962), Nafe and Drake (1963, p. 807), Bateman and Eaton (1967), and Hill (1978, p. 167).

The resultant model reproduces the observed gradient and amplitude of the gravity anomaly. A near-vertical fault or contact is required to produce the observed gradient SW. of point 2B (plate 1). The vertical fault is placed at -0.4 km (-0.2 mi) (fig. 20) and has a moderate density contrast of 0.30 g/cm^3. The overall model depicts a horst or structural high in the basement rocks from about -0.4 to 5.0 km (-0.2 to 3.1 mi) (fig. 20) and at depths from about sea-level to 0.8 km (0.5 mi) below sea-level. The horst and probable faults are shown in a schematic representation of the geology (fig. 21).

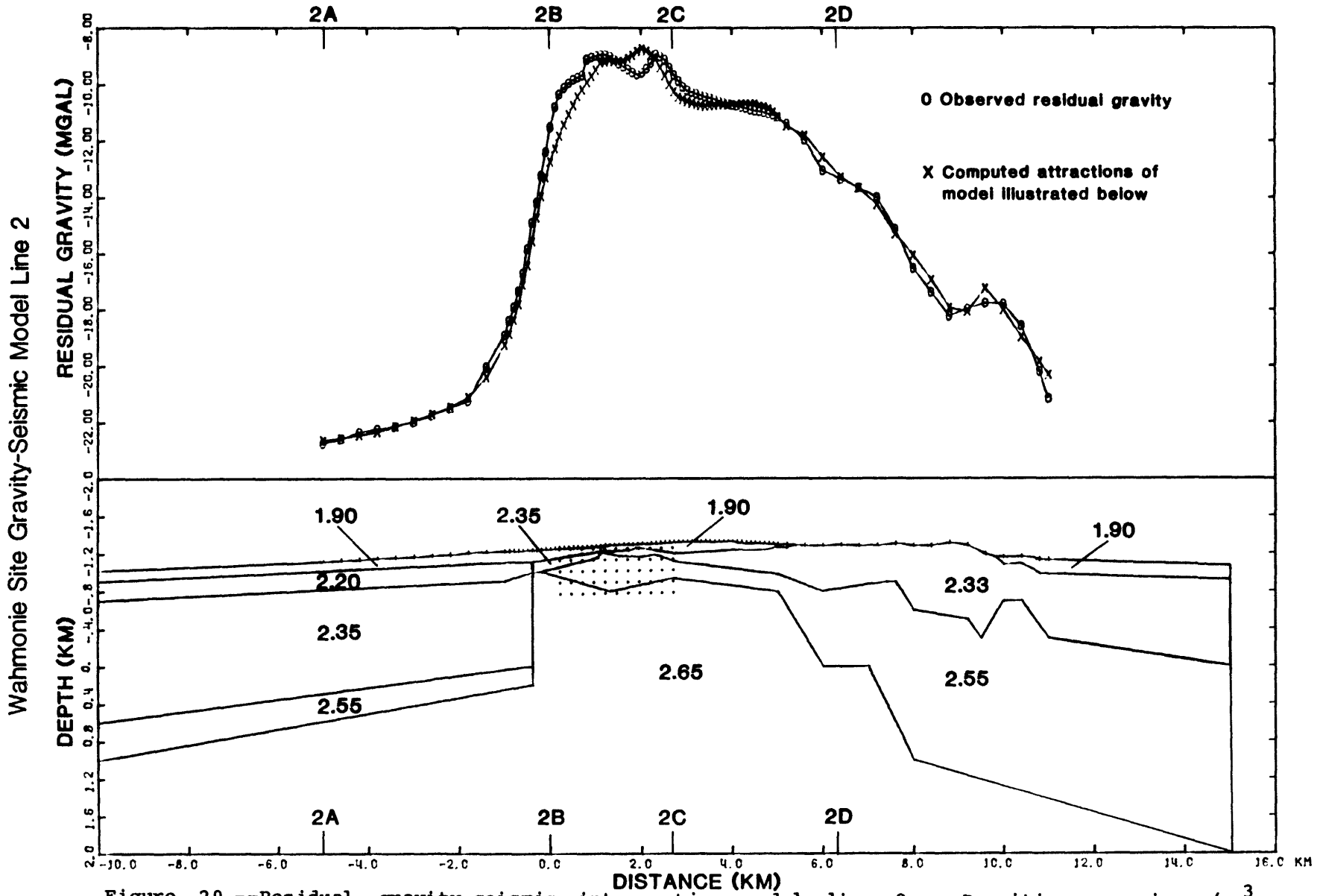

Figure 20.--Residual gravity-seismic interpretive model line 2. Densities are in g/cm^3. Stippled area denotes seismic refraction control. The profile is located on plate 1. A schematic of the geology is shown in figure 21.

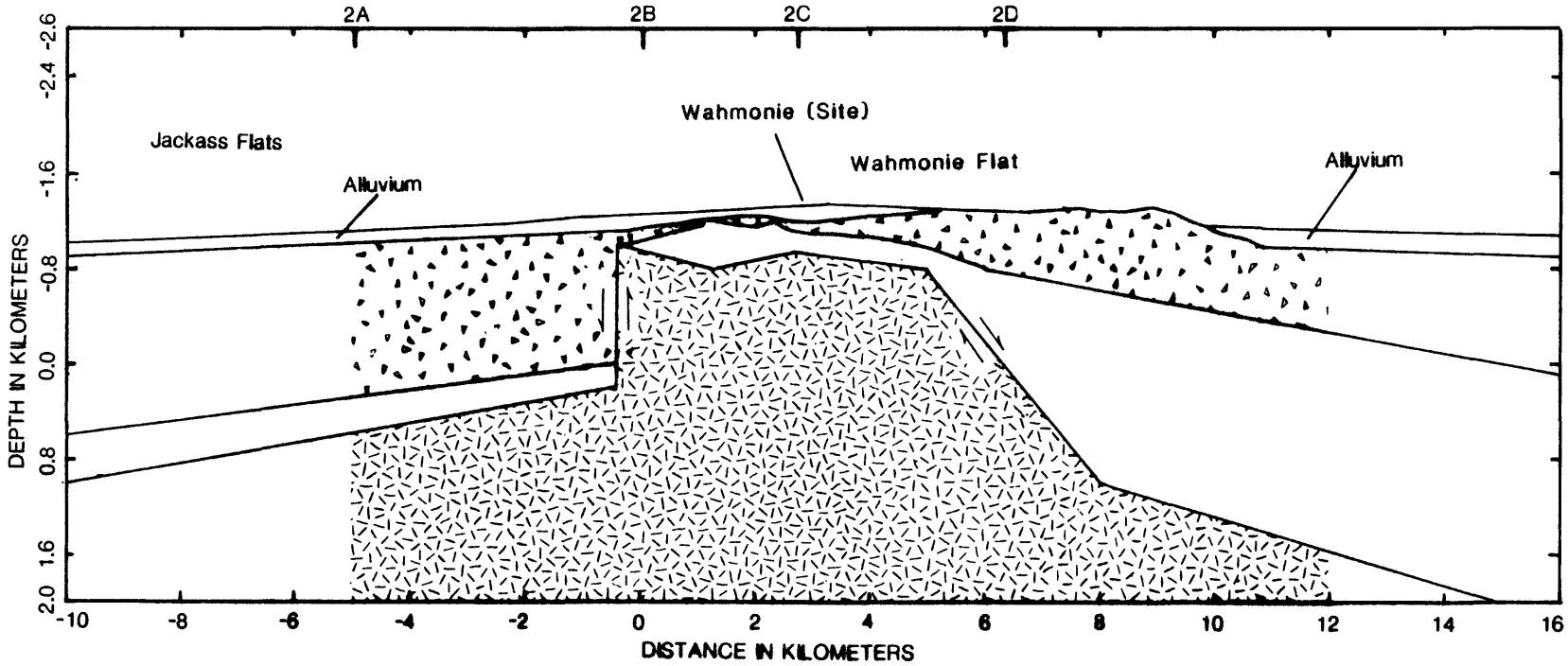

Figure 21.--Schematic of the geology represented in model line 2, figure 20.

Although gravity and magnetic evidence suggests that a cupola of the intrusive body may be shallow in the vicinity of Wahmonie Site, the seismic profile (fig. 15) does not detect rocks with velocities greater than 5.0 km/sec (16,400 ft/sec) to a depth of 550 m (1,800 ft) as would be expected for a felsic intrusive. The gravity model, based on the seismic data, also shows no anomalous mass necessary to produce the observed gravity profile other than the bodies suggested by the seismic model. However, the third velocity group, with a density of 2.55 g/cm^3 could represent an intensely altered or fractured portion of the intrusive body rather than an altered argillite member of the Eleana Formation (table 4). Electrical data suggest that this is possible because the resistivity begins to increase downward at depths as shallow as 50 m (160 ft) near Wahmonie Site (D. B. Hoover, written commun., 1980).

West-East Gravity Model Line 3

A third gravity model line begins in eastern Jackass Flats, strikes N.90°E., crosses Wahmonie Flat, and ends in western Frenchman Flat (plate 1, line 3). The interpreted model along profile line 3A-3B is primarily based on a projection of the seismic model (line 2B-2C) and is shown in figure 22. Alluvial deposits represented by bodies with a density of 1.90 g/cm^3 in Jackass Flats thicken westward of Wahmonie Site to about 150 m (500 ft). Hydrothermally altered rocks of the Wahmonie Formation that crop out along the profile have a density of 2.35 g/cm^3. Fractured granitic rocks, rhyodacite, or altered argillite of the Eleana Formation are represented by a 2.55 g/cm^3 body below the hydrothermally altered rocks. The inferred intrusive body is shown with a density of 2.65 g/cm^3. The geology of the model is shown schematically in figure 23.

The observed and calculated gravity anomaly curves agree well. The steep western gradient is produced by a vertical fault at a distance of -2.2 km (-1.4 mi) (fig. 22) which has a density contrast of 0.30 g/cm^3. The fault lies near the outer edge of the zone of hydrothermal alteration, where several north-trending faults are mapped on the geologic base (plate 1). This fault also correlates well with the inferred fault depicted on the gravity-seismic model (fig. 20).

Gravity-Seismic Model Line 4

Profile line 4A-4D begins in northwest Wahmonie Flat, strikes N.90°E.,and crosses the Wahmonie horst and the southern granodiorite exposure (plate 1). A preliminary gravity model is shown in figure 24 with a schematic representation of the geology in figure 25. The central part of the model (4B-4C) is based on the seismic refraction

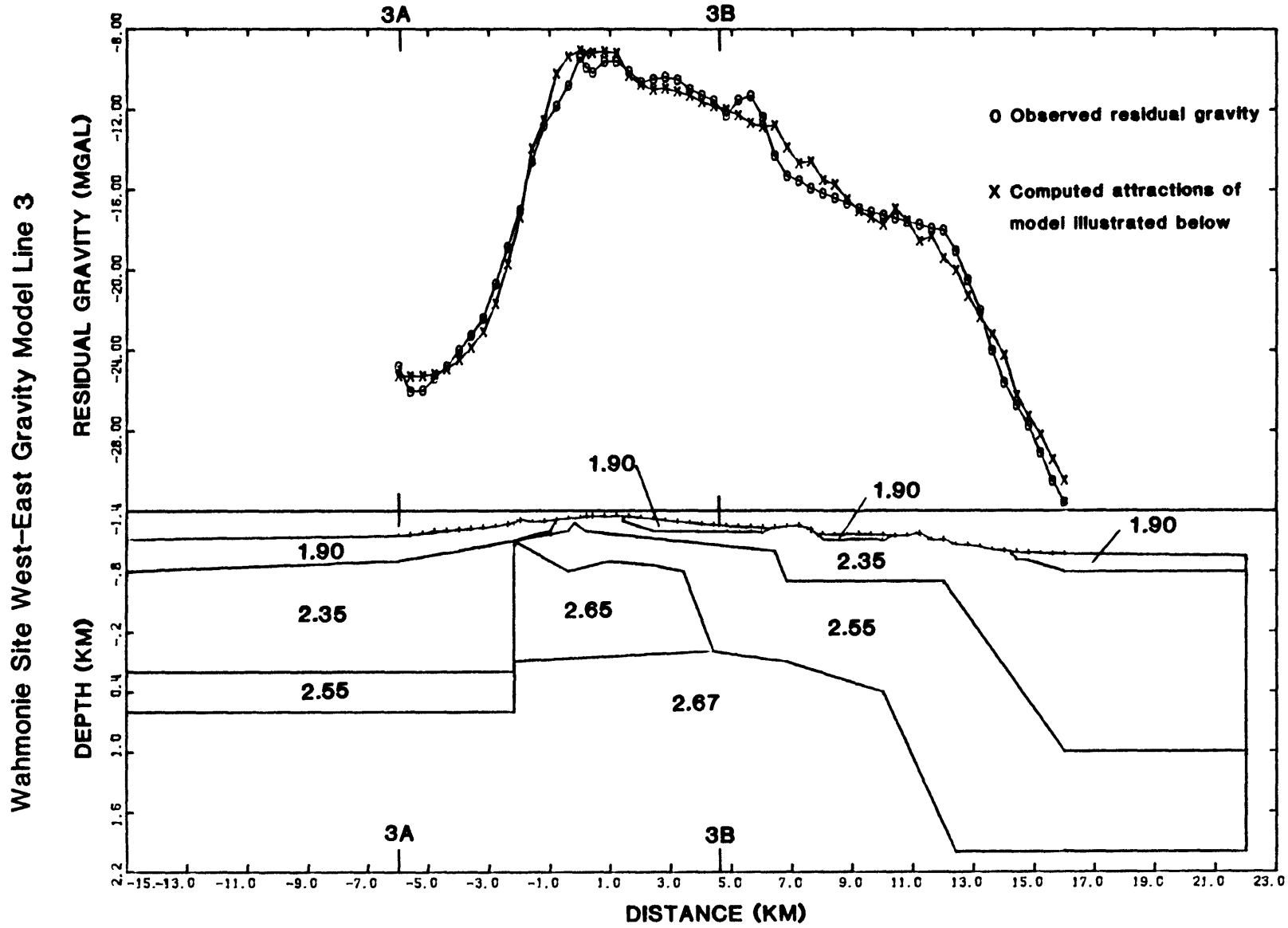

Figure 22.--West-east residual gravity anomaly interpretive model line 3. Densities are in g/cm^3. The profile is located on plate 1. A schematic of the geology is shown in figure 23.

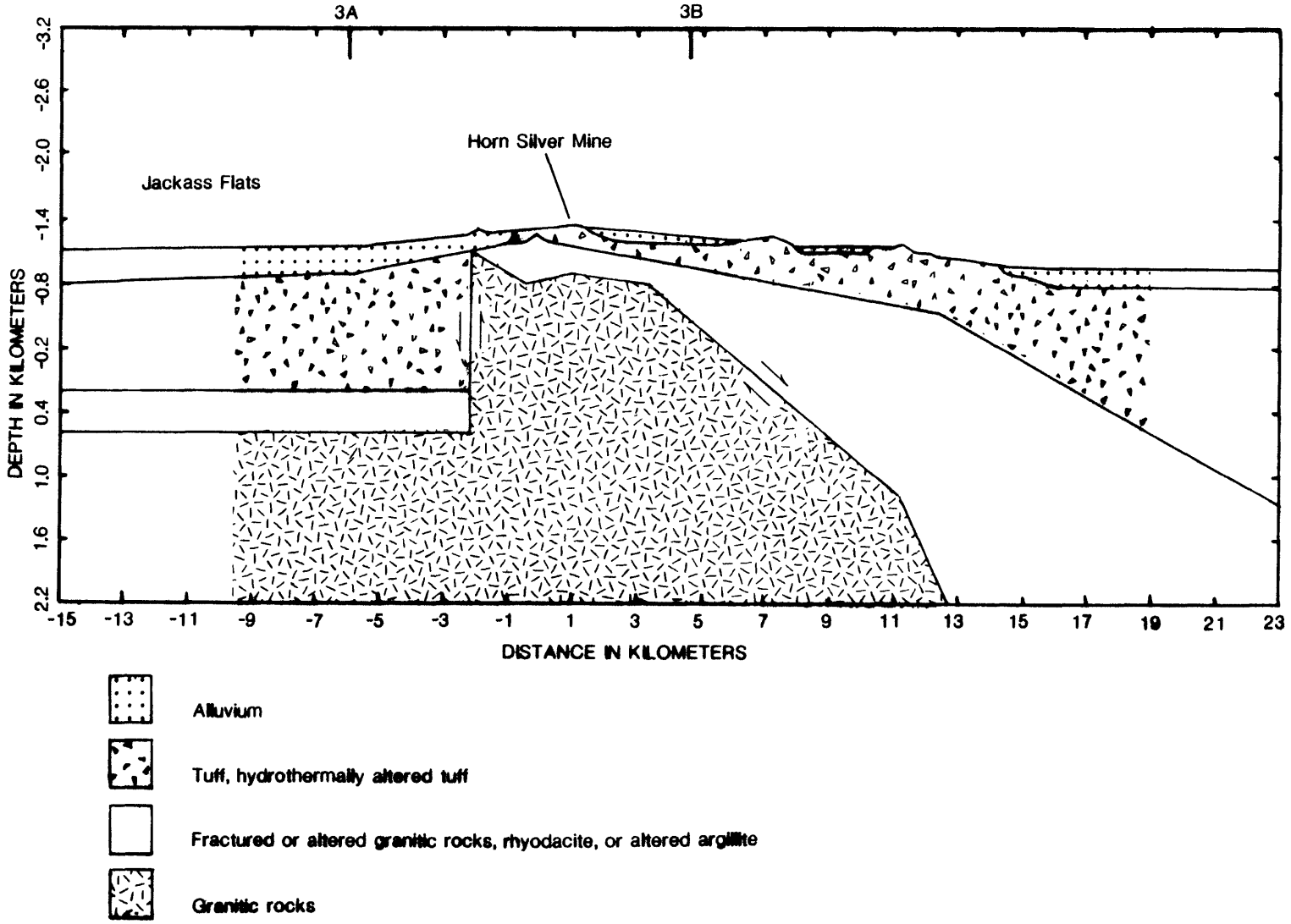

Figure 23.--Schematic of the geology represented in model line 3, figure 22.

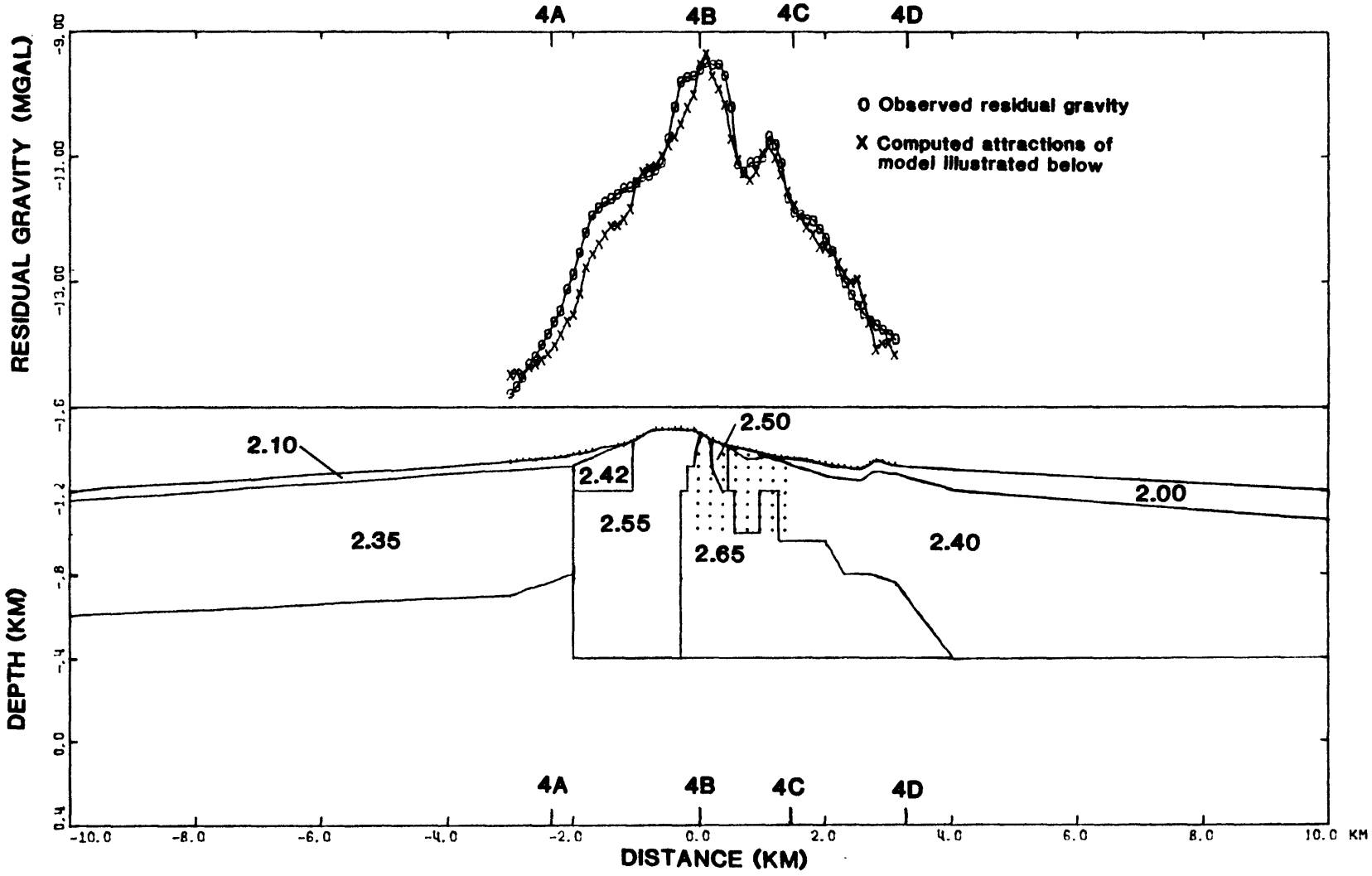

Figure 24.--Residual gravity-seismic interpretive model line 4. Densities are in g/cm^3. Stippled area denotes area of seismic refraction control. The profile is located on plate 1. A schematic of the geology is shown in figure 25.

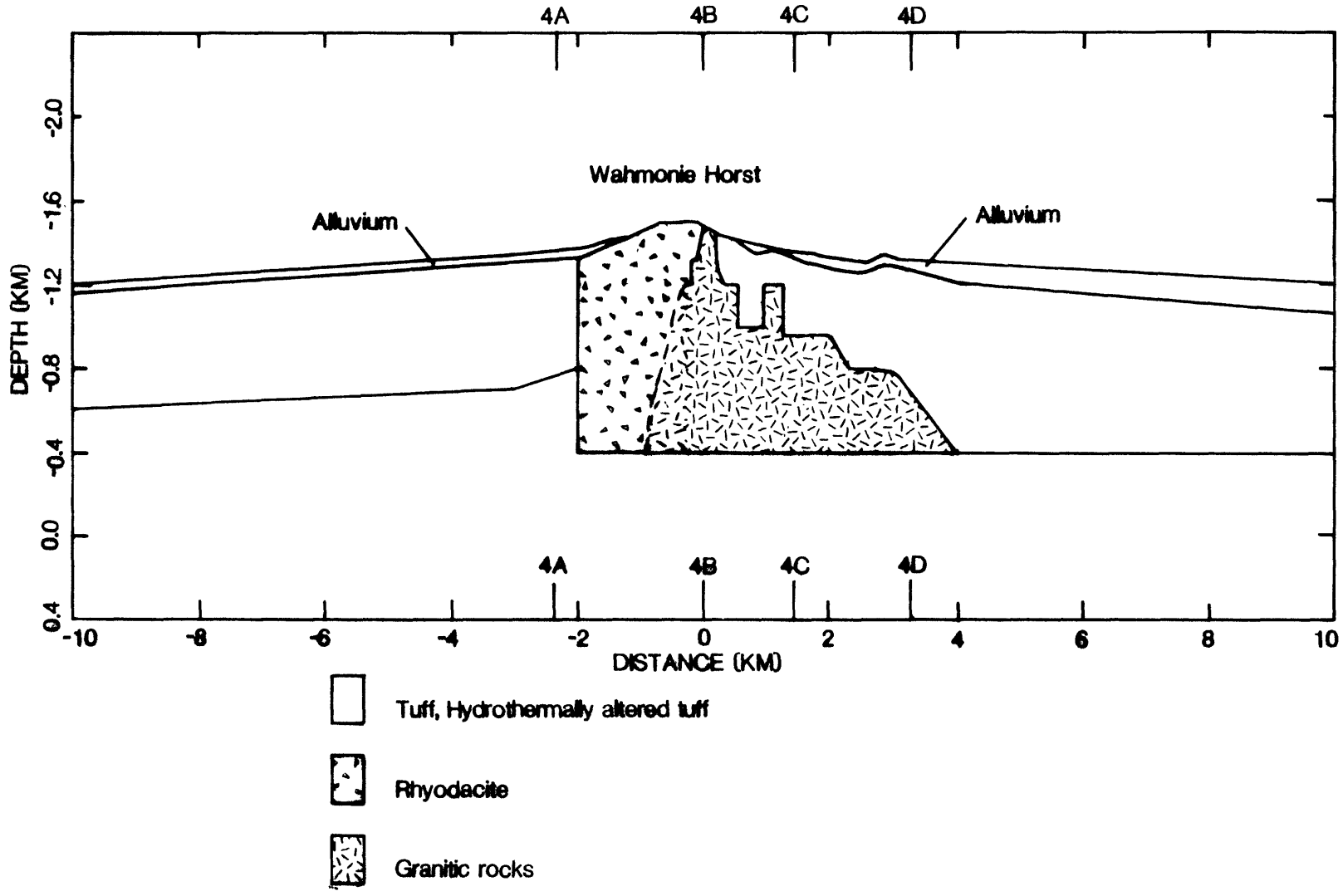

Figure 25.--Schematic of the geology represented in model line 4, figure 24.

model (fig 17) by L. W. Pankratz (written commun., 1981) which provides limited control from a distance of 0.0 to 1.4 km (0.0 to 0.87 mi) and to an elevation of 1,000 m (3,280 ft). Alluvial deposits are represented by bodies with densities of 2.00 and 2.10 g/cm^3. Other density values were determined by rock sampling and are consistent with velocity to density conversions of Nafe and Drake (1963, p. 807) and Hill (1978, p. 167).

Although high seismic velocities near 5.0 km/sec (16,000 ft/sec) were not detected near the granodiorite outcrop (fig. 17) the gravity data indicate the presence of a moderately high density body. This discrepancy between the seismic and gravity data may be due to starting the seismic spread too close to the edge of the granitic body or to weathering of the granitic rocks (L. W. Pankratz, written commun., 1981). The gravity model and the seismic data show the granodiorite body extending east of its surface outcrop, about 200 m (700 ft) below the surface to a distance of 1.1 km (0.68 mi) (fig. 24). A smaller gravity high at about 1.1 km (0.68 mi) may represent a cupola (?) of high density material.

A geologic cross-section by Ekren and Sargent (1965) show the granodiorite body extending only to the west of its surface exposure at depth whereas the gravity and seismic data suggest that the granitic body extends east at least 900 m (3,000 ft) and probably also extends to the west based on gravity data. Steep gravity gradients at the west edge of the granodiorite outcrop and at the west edge of the Wahmonie horst are probably caused by near-vertical contacts or faults were rocks of differing density are juxtaposed.

CONCLUSIONS

Gravity anomalies show excellent correlation with aeromagnetic, ground magnetic, and seismic anomalies. Magnetic information includes a 120-meter (400-foot) drape aeromagnetic survey and a ground magnetic traverse (line 1B-1C). Seismic data include a fan shot across eastern Jackass Flats (fig. 7, line SS') a seismic refraction profile across Wahmonie Site (plate 1, line 2B-2C), and a seismic refraction profile across the southern granodiorite body (plate 1, line 4B-4C). Other information includes electric methods, rock sampling, and the lithologic correlation to seismic velocities and core densities in drill hole UE25a-3 in Calico Hills.

The gravity interpretation suggests that altered tuffaceous rocks or rocks of the Eleana Formation are intruded by a granodiorite body. The outer zone of hydrothermal alteration appears approximately to mark the limit of the intrusive body. A prominent fault located at the west edge of the inferred intrusive is revealed at -0.4 km (-0.2 mi) (fig. 19) and at -2.2 km (-1.4 mi) (fig. 20), near the outer edge of the zone of hydrothermal alteration. It is likely that altered or fractured granitic rocks or rhyodacite occur beneath the hydrothermally altered volcanic rocks at Wahmonie Site. However, these rocks, with a density of 2.55 g/cm^3, might also represent an altered argillite member of the Eleana Formation. Below the 2.55 g/cm^3 layer, a dense (2.65 g/cm^3) and magnetic body is probably a felsic pluton similar to and possibly contiguous with the granodiorite rocks that crop out in the Wahmonie horst. A less likely alternative is that the 2.65 g/cm^3 body represents an altered marble similar to that at Calico Hills.

Although geophysical evidence suggests the existence of a sufficient volume of intrusive rock beneath Wahmonie Site for a possible nuclear waste repository, geologic and structural control for the site is inadequate. Ultimately, a drilling program would be required to resolve the nature of velocity group three which may be a highly altered or fractured portion of a granitic intrusive, rhyodacite, or an altered argillite member of the Eleana Formation. The drilling program would also provide other geologic, structural, and density constraints for further gravity analysis.

A recommended drill-site location would be the center of the -9 mGal closed contour about 500 m (1,600 ft) south of the Horn Silver mine (plate 1). The gravity-seismic model along profile 2 (figs. 14, 18) suggests that the depth to a 2.65 g/cm^3 body (granodiorite?) is about 500 m (1,500 ft). However, a dense magnetic cupola (?) may be present in this area less than 200 m (600 ft) below the surface (figs. 12, 15). An alternate drill-site location would be the seismic refraction structural high located 1,200 m (3,900 ft) east of point 2B (fig. 14). Any drilling program in this area should be prepared to drill to a depth

of at least 1,500 m (5,000 ft) because of the inherent uncertainties in the potential field method. However, the probability is moderately high that granitic rocks would be reached at half that depth.

REFERENCES

Ball, S. H., 1907, A geologic reconnaissance in southwestern Nevada and eastern California: U.S. Geological Survey Bulletin 308, p. 146-147.

Barnes, Harley, 1967, Geologic description of selected rock samples from the Nevada Test Site: U.S. Geological Survey Technical Letter NTS-185, Prepared by the U.S. Geological Survey for the Defense Atomic Support Agency, 21 p.

Bateman, P. C. and Eaton, J. P., 1967, The Sierra Nevada batholith: Science, v. 158, p. 1407-1417.

Bath, G. D., 1968, Aeromagnetic anomalies related to remanent magnetism in volcanic rock, Nevada Test Site, in Eckel, E. B., ed., Nevada Test Site: Geological Society of America Memoir 110, p. 135-146.

Cady, J. W., 1980, Calculation of gravity and magnetic anomalies of finite-length right polygonal prisms: Geophysics, v. 45, no. 10, p. 1507-1512.

Carr, W. J., Bath, G. D., Healey, D. L., and Hazelwood, R. M., 1975, Geology of northern Frenchman Flat, Nevada Test Site: U.S. Geological Survey Technical Letter NTS-188, Prepared by the U.S. Geological Survey for the Nevada Operations Office, U.S. Energy Research and Development Administration, 24 p.

Cordell, Lindrith, and Henderson, R. G., 1968, Iterative three-dimensional solution of gravity anomaly data using a digital computer: Geophysics, v. 33, no. 4, p. 596-601.

Cornwall, H. R., 1972, Geology and mineral deposits of southern Nye County, Nevada: Nevada Bureau of Mines and Geology Bulletin 77, 49 p.

Diment, W. H., Stewart, S. W., and Roller, J. C., 1961, Crustal structure from the Nevada Test Site to Kingman, Arizona, from seismic and gravity obsrvations: Journal Geophysical Research, v. 66, no. 1, p. 201-214.

Dobrin, M. B., 1960, Introduction to geophysical prospecting: New York, McGraw-Hill Book Co., 2nd ed., 446 p.

Eakin, T. E., Schoff, S. L., and Cohen, Philip, 1963, Regional hydrology of a part of southern Nevada--A reconnaissance: U.S. Geological Survey Trace Elements Investigations Report TEI-833, 40 p.

Ekren, E. B., Rogers, C. L., Anderson, R. E., and Orkild, P. P., 1968, Age of basin and range normal faults in Nevada Test Site and Nellis Air Force Range, Nevada, in Eckel, E. B., ed., Nevada Test Site: Geological Society of America Memoir 110, p. 247-250.

Ekren, E. B., and Sargent, K. A., 1965, Geologic map of the Skull Mountain quadrangle, Nye County, Nevada: U.S. Geological Survey Geologic Quadrangle Map GQ-387, scale 1:24,000.

Hazelwood, R. M., Healey, D. L., and Miller, C. H., 1963, U.S. Geological Survey investigations of Yucca Flat, Nevada Test Site, Part B--Geophysical Investigations: U.S. Geological Survey Technical Letter NTS-45, Prepared by the U.S. Geological Survey for the U.S. Atomic Energy Commission, 53 p.

Healey, D. L., 1967, Borehole gravity meter observations in drill hole Ue19n, Pahute Mesa, Nevada Test Site: U.S. Geological Survey Technical Letter I-55, Prepared by the U.S. Geological Survey for the U.S. Atomic Energy Commission, 10 p.

Healey, D. L., and Miller, C. H., 1962, Gravity survey of the Nevada Test Site and vicinity, Nye, Lincoln, and Clark Counties, Nevada--Interim report: U.S. Geological Survey Trace Elements Investigations Report TEI-827, 36 p.

Hill, D. P., 1978, Seismic evidence for the structure and Cenozoic tectonics of the Pacific Coast States, in Smith, R. B., and Eaton, G. P., eds., Cenozoic tectonics and regional geophysics of the western Cordillera: Geological Society of America Memoir 152, p. 145-174.

International Union of Geodesy and Geophysics, 1971, Geodetic reference system 1967: International Association of Geodesy Special Publication no. 3, 116 p.

Izett, G. A., 1960, "Granite" exploration hole, Area 15, Nevada Test Site, Nye County, Nevada--Interim report, Part C, Physical properties: U.S. Geological Survey Trace Elements Memorandum Report 836-C, 36 p.

Johnson, M. S., and Hibbard, D. E., 1957, Geology of the Atomic Energy Commission Nevada Proving Grounds area, Nevada: U.S. Geological Survey Bulletin 1021-K, p. 333-384.

Johnson, R. B., Ege, I R., 1964, Geology of the Pluto Site, Area 401, Nevada Test Site, Nye County, Nevada: U.S. Geological Survey Trace Elements Investigations Report TEI-841, 127 p.

Keller, G. V., 1959, Porosity, density, and fluid permeability of the Oak Spring Formation, in Diment, W. H., and others, Properties of the Oak Spring Formation in Area 12 at the Nevada Test Site: U.S. Geological Survey Trace Elements Investigations Report TEI-672.

Kistler, R. W., 1968, Potassium argon ages of volcanic rocks in Nye and Esmeralda Counties, Nevada, in Eckel, E. B., ed., Nevada Test Site: Geological Society of America Memoir 110, 251-262.

Kral, V. E., 1951, Mineral resources of Nye County, Nevada: Nevada University Bulletin, v. 45, no. 3, Geology and Mining Series no. 50, 222 p.

Maldonado, Florian, Muller, D. C., and Morrison, J. N., 1979, Preliminary geologic and geophysical data of the UE25a-3 exploratory drill hole, Nevada Test Site, Nevada: U.S. Geological Survey Report USGS-1543-6: available from National Technical Information Service, U.S. Department of Commerce, Springfield, VA, 22152, 47 p.

Moore, J. E., 1962, Selected logs and drilling records of wells and test holes at the Nevada Test Site prior to 1960: U.S. Geological Survey Trace Elements Investigations Report TEI-804, 54 p.

Morelli, C. (Ed.), 1974, The International Gravity Standardization Net, 1971: International Association of Geodesy Special Publication no. 4, 194p.

Nafe, J. W., and Drake, C. L., 1963, Physical properties of marine sediments, in Hill, M. N., ed., The sea, v. 3: New York, Interscience, p. 794-815.

Nettleton, L. L., 1940, Geophysical prospecting for oil: New York, McGraw-Hill Book Co., 1st ed., 444 p.

Orkild, P. P., 1964, Paintbrush Tuff and Timber Mountain Tuff of Nye County, Nevada, in Changes in stratigraphic nomenclature by the U.S. Geological Survey, 1964: U.S. Geological Survey Bulletin 1224-A, p. A44-A51.

Plouff, Donald, 1966, Digital terrain corrections based on geographic coordinates [abs.]: Geophysics, v. 31, no. 6, p. 1208.

Plouff, Donald, 1977, Preliminary documentation for a FORTRAN program to compute gravity terrain corrections based on topography digitized on a geographic grid: U.S. Geological Survey Open-File Report 77-535, 45 p.

Poole, F. G., Carr, W. J., and Elston, D. P., 1965, Salyer and Wahmonie Formations of southeastern Nye County, Nevada, in Changes in stratigraphic nomenclature by the U.S. Geological Survey, 1964: U.S. Geological Survey 1224-A, p. A36-A44.

Poole, F. G., Elston, D. P., and Carr, W. J., 1965, Geologic map of the Cane Spring quadrangle, Nye County, Nevada: U.S. Geological Survey Quadrangle Map GQ-455, scale 1:24,000.

Robbins, S. L., Oliver, H. W., Holden, K. D., and Farewell, R. C., 1974, Principal facts, accuracies, and sources for 3046 gravity stations on the San Jose 1 degree x 2 degree quadrangle, California: available from National Technical Information Service, U.S. Department of Commerce, Springfield, VA 22152, PB-232728, 32 p.

Ross, C. S., and Smith, R. L., 1961, Ash-flow tuffs: Their origin, geologic relations, and identification: U.S. Geological Survey Professional Paper 366, 81 p.

Snyder, D. B., and Oliver, H. W., 1980, Preliminary results of gravity investigations of the Calico Hills, Nevada Test Site, Nye County, Nevada: U.S. Geological Survey Open-File Report 81-101 42 p.

Swick, C. A., 1942, Pendulum gravity measurements and isostatic reductions: U.S. Coast and Geodetic Survey Special Publication 232, 82 p.

Talwani, Manik, Worzel, J. L., and Landisman, Mark, 1959, Rapid gravity computations for two-dimensional bodies with application to the Mendocino submarine fracture zone: Journal Geophysical Research, v. 64, no. 1, p. 49-59.

Talwani, Manik, and Ewing, Maurice, 1960, Rapid computation of gravitational attraction of three-dimensional bodies of arbitrary shape: Geophysics, v. 25, no. 1, p. 302-225.

Tanner, J. G., 1967, An automated method of gravity interpretation: Geophysics Journal Research Astronomical Society, v. 13, p. 339-347.

U.S. Geological Survey, 1979, Aeromagnetic map of the Timber Mountain Area, Nevada: U.S. Geological Survey Open-File Report 79-587, scale 1:62,500, 3 sheets.

Vacquier, Victor, Steenland, Clarence, Anderson, R. G., and Zeitz, Isidore, 1951, The interpretation of aeromagnetic maps: Geological Society of America Memoir 47, 151 p.

Winograd, I. J., 1962, Interbasin movement of ground water at the Nevada Test Site, Nevada: U.S. Geological Survey Professional Paper 450-C, p. C108-C111.

Winograd, I. J., and Thordarson, William, 1975, Hydrogeologic and hydrochemical framework, South-Central Breat Basin, Nevada-California, with special reference to the Nevada Test Site: U.S. Geological Survey Professional Paper 712-C, 126 p.

Woollard, G. P., 1962, The relation of gravity anomalies to surface elevation, crustal structure, and geology: Aeronautical Chart and Information Center Research Report Series, no. 62-9, 292 p.

APPENDIX

Principal facts for gravity stations on the Skull Mountain 7½ minute quadrangle, Nye County, Nevada. STAT is the gravity station name. LAT (latitude) and LONG (longitude) are expressed in degrees and decimal minutes. ELEV is the station elevation and is reported to the nearest foot. OG is the observed gravity in mGal. TC, the terrain correction in mGal, is calculated to a radial distance of 166.7 km (103.6 mi). FAA is the free-air anomaly in mGal. CBA1 and CBA2 are the complete Bouguer anomalies in mGal reduced for densities of 2.67 and 2.50 g/cm^3, respectfully.

STAT NAME	LAT deg	min	LONG deg	min	ELEV feet	OG mGal	TC mGal	FAA mGal	CBA1 2.67	CBA2 2.50
253	36	45.28	116	8.02	4248	979486.37	1.77	2.35	-142.07	-132.88
254	36	45.43	116	8.02	4268	979485.56	1.79	3.21	-141.88	-132.64
255	36	45.58	116	8.02	4356	979480.17	1.97	5.87	-142.05	-132.63
256	36	45.73	116	8.02	4446	979474.49	2.06	8.44	-142.48	-132.87
257	36	45.90	116	8.02	4472	979473.98	2.07	10.13	-141.67	-132.00
258	36	46.02	116	8.00	4411	979478.66	2.08	8.90	-140.80	-131.26
259	36	46.15	116	8.00	4517	979472.14	2.30	12.15	-140.95	-131.21
260	36	46.33	116	8.00	4590	979467.19	2.50	13.80	-141.61	-131.71
261	36	46.48	116	8.00	4556	979471.87	2.53	15.07	-139.14	-129.32
262	36	46.63	116	8.00	4665	979466.00	3.04	19.23	-138.21	-128.18
288	36	46.80	116	8.00	4751	979460.07	3.86	21.14	-138.42	-128.26
289	36	46.92	116	8.00	4701	979463.74	3.52	19.94	-138.25	-128.18
290	36	47.05	116	8.00	4705	979463.85	3.52	20.24	-138.09	-128.01
291	36	47.18	116	8.00	4742	979461.04	3.59	20.71	-138.81	-128.65
332	36	45.48	116	10.16	4727	979454.96	3.59	15.68	-143.33	-133.20
333	36	45.70	116	9.73	4863	979445.42	5.29	18.61	-143.36	-133.04
334	36	45.78	116	9.22	5008	979432.92	7.35	19.63	-145.24	-134.75
335	36	45.53	116	9.15	4785	979446.82	4.81	12.92	-146.85	-136.68
1123	36	52.42	116	9.66	4687	979460.69	1.50	7.62	-152.11	-141.94
1124	36	52.03	116	9.50	4773	979456.86	1.79	12.44	-149.95	-139.61
1125	36	51.75	116	9.13	4795	979459.72	1.51	17.77	-145.65	-135.24
1126	36	51.40	116	8.70	4846	979458.75	2.10	22.10	-142.47	-132.00
1127	36	51.02	116	8.67	4727	979465.81	1.79	18.53	-142.28	-132.05
1128	36	50.62	116	8.47	4551	979474.71	1.56	11.46	-143.55	-133.69
1129	36	50.22	116	8.22	4438	979481.39	1.27	8.09	-143.34	-133.70
1130	36	49.87	116	7.97	4319	979489.21	1.09	5.23	-142.30	-132.91
1131	36	49.48	116	7.75	4218	979495.73	1.04	2.82	-141.30	-132.12
1136	36	49.12	116	7.62	4131	979502.47	1.23	1.90	-139.05	-130.07
1137	36	49.02	116	8.13	4194	979499.35	1.15	4.85	-138.34	-129.22
1138	36	48.95	116	8.67	4257	979496.60	1.30	8.13	-137.07	-127.83
1139	36	49.10	116	9.32	4358	979489.86	1.15	10.66	-138.15	-128.67
1140	36	48.90	116	9.58	4358	979490.23	1.04	11.33	-137.59	-128.11
1141	36	48.67	116	10.04	4272	979496.54	0.99	9.88	-136.14	-126.85
1142	36	48.53	116	10.55	4212	979499.99	1.19	7.89	-135.87	-126.72
1143	36	48.47	116	11.03	4158	979503.01	1.17	5.92	-136.02	-126.98
1144	36	48.52	116	11.57	4130	979502.04	1.05	2.25	-138.85	-129.87
1145	36	48.68	116	12.08	4098	979497.35	0.93	-5.68	-145.80	-136.88
1146	36	48.95	116	12.53	4080	979496.33	1.03	-8.79	-148.19	-139.31
1147	36	49.25	116	12.87	4081	979495.90	1.02	-9.56	-149.00	-140.12
1148	36	49.47	116	13.22	4052	979496.16	1.01	-12.33	-150.80	-141.98
1149	36	49.75	116	13.63	3989	979499.94	1.09	-14.89	-151.11	-142.44
1150	36	49.98	116	14.07	3958	979502.15	1.19	-15.92	-150.98	-142.38
1151	36	50.38	116	14.42	3994	979499.13	1.30	-16.14	-152.32	-143.65
1152	36	50.68	116	14.80	4016	979497.35	1.20	-16.28	-153.32	-144.59
1177	36	52.07	116	13.05	4519	979471.26	1.62	2.90	-150.96	-141.16

STAT NAME	LAT deg	min	LONG deg	min	ELEV feet	OG mGal	TC mGal	FAA mGal	CBA1 2.67	CBA2 2.50
1178	36	51.58	116	13.67	4314	979482.74	1.73	-4.18	-150.90	-141.56
1271	36	51.03	116	14.57	4138	979491.37	1.35	-11.30	-152.36	-143.38
1523	36	47.55	116	14.95	3624	979521.29	0.82	-24.67	-148.64	-140.75
1524	36	47.62	116	14.37	3692	979517.41	0.83	-22.26	-148.55	-140.51
1525	36	47.75	116	13.95	3759	979513.75	0.84	-19.81	-148.39	-140.20
1526	36	47.03	116	13.42	3835	979510.09	0.86	-15.28	-146.45	-138.10
1527	36	47.15	116	12.92	3908	979505.45	0.88	-13.23	-146.88	-138.37
1528	36	48.17	116	12.48	3983	979501.47	0.88	-11.64	-147.86	-139.19
1529	36	48.38	116	12.22	4063	979499.53	0.91	-6.36	-145.30	-136.45
1636	36	45.20	116	11.53	5714	979383.63	12.60	37.53	-146.23	-134.53
1637	36	45.93	116	11.33	5768	979380.45	12.74	38.38	-147.10	-135.29
1638	36	46.57	116	10.48	5975	979365.69	17.07	42.14	-146.08	-134.09
1640	36	46.80	116	9.54	5751	979387.89	12.49	42.95	-142.19	-130.40
1641	36	47.02	116	9.29	5671	979394.19	10.83	41.42	-142.65	-130.93
1642	36	47.42	116	8.66	5697	979390.20	12.66	39.30	-143.83	-132.17
1643	36	47.78	116	8.22	5304	979421.24	6.74	32.88	-142.73	-131.55
1644	36	45.68	116	14.98	3546	979526.57	1.01	-24.02	-145.13	-137.41
1646	36	46.12	116	14.65	3581	979524.31	1.02	-23.62	-145.92	-138.13
1647	36	46.55	116	14.10	3676	979518.98	1.15	-20.64	-146.07	-138.08
1648	36	46.98	116	14.55	3765	979514.40	1.18	-17.48	-145.93	-137.75
1649	36	47.55	116	12.73	3900	979507.99	1.20	-12.02	-145.08	-136.61
1650	36	47.83	116	12.20	3990	979503.84	1.23	-8.12	-144.23	-135.56
1651	36	48.00	116	11.72	4075	979503.14	1.26	-1.07	-140.07	-131.22
1652	36	48.30	116	10.53	4245	979498.07	1.32	9.41	-135.36	-126.14
1653	36	49.03	116	14.73	3769	979511.00	0.84	-23.47	-152.40	-144.19
1654	36	49.15	116	14.40	3837	979506.53	0.95	-21.72	-152.87	-144.52
1657	36	51.03	116	14.58	4138	979491.77	1.35	-10.90	-151.97	-142.99
1658	36	51.82	116	13.95	4366	979479.91	1.64	-2.46	-151.06	-141.60
1659	36	52.37	116	14.97	4745	979454.21	3.30	6.67	-153.25	-143.07
1660	36	51.77	116	14.88	4281	979484.44	1.60	-5.86	-151.58	-142.30
1661	36	51.28	116	12.98	4959	979439.29	3.42	13.43	-153.69	-143.05
1663	36	49.90	116	12.68	4376	979476.68	1.92	-1.98	-150.64	-141.18
1664	36	49.60	116	11.73	4587	979469.19	5.22	10.79	-141.79	-132.08
1665	36	49.47	116	12.13	4438	979476.73	2.95	4.52	-145.23	-135.69
1669	36	50.33	116	11.90	4795	979454.59	4.18	14.70	-146.05	-135.82
1670	36	50.48	116	11.07	4729	979461.54	2.37	15.22	-145.08	-134.87
1688	36	51.32	116	10.03	5651	979398.88	8.67	38.01	-147.53	-135.72
1689	36	51.57	116	10.22	5514	979406.15	6.73	32.04	-150.76	-139.12
1690	36	51.75	116	10.57	5478	979406.91	6.47	29.16	-152.67	-141.09
1691	36	52.05	116	10.72	5142	979431.91	3.56	22.15	-151.10	-140.07
1692	36	52.42	116	10.80	5088	979434.82	3.27	19.44	-152.25	-141.31
1705	36	49.27	116	10.04	4632	979473.88	1.76	20.20	-137.39	-127.36
1706	36	49.98	116	9.79	5361	979420.81	9.57	34.62	-140.10	-128.98
1707	36	49.72	116	10.13	5081	979442.04	5.12	29.91	-139.69	-128.89
1708	36	49.08	116	10.55	4435	979486.65	1.31	14.72	-136.57	-126.94

STAT NAME	LAT deg	min	LONG deg	min	ELEV feet	OG mGal	TC mGal	FAA mGal	CBA1 2.67	CBA2 2.50
1709	36	48.70	116	9.57	4303	979494.35	1.12	10.56	-136.39	-127.04
1743	36	49.35	116	7.62	4178	979499.58	1.02	3.10	-139.67	-130.58
1744	36	49.58	116	7.67	4244	979493.55	1.28	2.94	-141.83	-132.62
1745	36	49.65	116	8.02	4288	979491.61	1.08	5.04	-141.45	-132.12
1746	36	49.77	116	7.58	4452	979479.48	2.48	8.16	-142.55	-132.95
1747	36	50.07	116	7.58	4349	979486.00	1.97	4.56	-143.13	-133.72
1748	36	50.95	116	8.40	4901	979448.88	3.90	18.05	-146.61	-136.12
1749	36	48.98	116	8.15	4211	979498.88	1.16	6.04	-137.73	-128.57
1750	36	49.10	116	8.62	4271	979495.11	1.20	7.73	-138.05	-128.76
1751	36	49.20	116	8.02	4207	979497.86	1.15	4.32	-139.32	-130.17
1752	36	49.45	116	8.03	4255	979494.89	1.07	5.50	-139.86	-130.60
1753	36	49.52	116	8.41	4333	979489.94	1.22	7.78	-140.10	-130.68
1754	36	49.92	116	8.57	4453	979482.39	1.28	10.94	-141.00	-131.32
1755	36	49.82	116	8.88	4489	979481.64	1.31	13.72	-139.42	-129.67
1756	36	49.47	116	8.98	4430	979484.87	1.29	11.90	-139.23	-129.61
1757	36	48.52	116	9.48	4368	979489.56	1.81	12.14	-136.35	-126.89
1758	36	48.98	116	8.13	4330	979491.93	1.22	10.27	-137.51	-128.10
1764	36	50.43	116	9.50	4903	979455.24	3.72	25.35	-139.55	-129.05
1765	36	50.32	116	9.83	5213	979434.49	5.35	33.90	-139.98	-128.91
1767	36	47.57	116	10.60	4568	979474.74	3.85	17.50	-135.81	-126.05
1768	36	47.47	116	10.22	4755	979462.19	3.58	22.66	-137.31	-127.13
1769	36	47.43	116	9.75	4732	979464.23	3.01	22.61	-137.15	-126.98
1770	36	47.68	116	9.63	4612	979472.32	2.57	19.05	-137.04	-127.10
1771	36	47.97	116	9.37	4629	979471.67	2.79	19.58	-136.87	-126.91
1772	36	48.10	116	9.95	4384	979488.70	1.83	13.39	-135.63	-126.14
1773	36	47.97	116	10.53	4365	979489.50	1.51	12.59	-136.10	-126.63
1812	36	51.98	116	9.29	5015	979441.07	2.13	19.47	-150.86	-140.02
1813	36	52.07	116	9.04	5054	979436.97	2.49	18.90	-152.40	-141.50
1814	36	52.23	116	8.78	4797	979452.33	1.60	9.87	-153.52	-143.12
1815	36	52.12	116	8.23	4850	979451.52	2.07	14.21	-150.53	-140.04
1816	36	52.05	116	7.78	4743	979458.20	2.20	10.93	-150.02	-139.77
1817	36	51.67	116	7.80	4900	979446.89	3.21	14.93	-150.39	-139.86
1818	36	51.72	116	8.13	5102	979433.42	4.18	20.37	-150.88	-139.98
1819	36	51.47	116	8.41	5136	979431.96	5.10	22.47	-149.03	-138.11
1820	36	51.73	116	8.50	5016	979441.07	3.55	19.92	-149.02	-138.26
1821	36	51.97	116	8.65	4949	979445.59	2.72	17.80	-149.68	-139.01
1822	36	51.63	116	12.50	4805	979452.87	2.62	12.03	-150.62	-140.26
1823	36	51.48	116	12.17	4905	979448.71	3.14	17.49	-148.06	-137.52
1824	36	51.43	116	11.85	5285	979420.65	4.41	25.22	-152.07	-140.78
1825	36	51.38	116	11.58	5399	979413.86	4.97	29.22	-151.41	-139.91
1827	36	51.75	116	11.67	5245	979423.71	4.35	24.06	-151.92	-140.71
1828	36	52.00	116	12.32	4917	979447.42	2.92	16.58	-149.61	-139.03
1890	36	48.05	116	7.50	5186	979425.82	6.67	25.97	-145.67	-134.74
1893	36	48.53	116	10.16	4232	979499.11	1.20	8.89	-135.55	-126.36
1894	36	48.92	116	12.62	4068	979497.27	1.03	-8.93	-147.92	-139.07

STAT NAME	LAT deg	min	LONG deg	min	ELEV feet	OG mGal	TC mGal	FAA mGal	CBA1 2.67	CBA2 2.50
1895	36	48.97	116	13.28	3979	979499.79	1.00	-14.85	-150.82	-142.16
1896	36	48.97	116	13.58	3938	979501.52	0.88	-16.97	-151.65	-143.08
1897	36	49.27	116	13.03	4065	979496.60	1.01	-10.39	-149.30	-140.45
1898	36	49.73	116	12.08	4346	979484.72	1.57	3.48	-144.50	-135.07
1899	36	50.67	116	10.50	4787	979461.10	1.86	19.96	-142.83	-132.47
1900	36	50.25	116	8.29	4448	979480.71	1.16	8.31	-143.57	-133.90
1901	36	50.42	116	8.33	4475	979479.21	1.39	9.10	-143.48	-133.76
1902	36	50.57	116	8.88	4695	979466.75	1.56	17.11	-142.84	-132.65
1903	36	51.53	116	8.91	4813	979461.00	1.75	21.06	-142.73	-132.31
1904	36	51.15	116	9.28	5123	979441.15	3.80	30.90	-141.46	-130.48
1905	36	51.20	116	8.95	5008	979448.49	2.36	27.36	-142.50	-131.69
1906	36	50.87	116	8.98	5082	979443.23	2.56	29.53	-142.66	-131.69
1907	36	50.97	116	9.63	5169	979439.31	4.29	33.65	-139.79	-128.75
1908	36	50.63	116	10.00	4975	979451.00	2.69	27.59	-140.81	-130.09
1909	36	50.28	116	10.16	4941	979453.22	3.10	27.12	-139.71	-129.09
1910	36	50.17	116	10.42	4721	979468.00	2.48	21.38	-138.54	-128.35
1911	36	49.38	116	10.33	4570	979478.39	1.61	18.72	-136.90	-126.99
1912	36	49.07	116	9.20	4365	979489.45	1.15	10.96	-138.09	-128.60
1913	36	49.40	116	9.17	4462	979483.07	1.31	13.22	-139.00	-129.31
1914	36	50.22	116	8.66	4585	979472.06	1.48	12.59	-143.67	-133.72
1915	36	50.50	116	7.70	4300	979490.51	1.18	3.83	-142.96	-133.61
1917	36	49.88	116	8.00	4323	979489.11	1.10	5.49	-142.17	-132.77
1918	36	49.35	116	7.58	4172	979499.30	1.02	2.26	-140.30	-131.23
1924	36	49.08	116	7.70	4141	979502.30	1.12	2.73	-138.68	-129.67
1925	36	49.03	116	8.00	4172	979500.46	1.14	3.88	-138.57	-129.50
1926	36	49.38	116	8.29	4286	979493.12	1.19	6.75	-139.56	-130.24
1927	36	49.67	116	8.50	4389	979486.74	1.25	9.64	-140.14	-130.60
1928	36	48.67	116	8.67	4336	979491.34	1.35	10.70	-137.16	-127.74
1929	36	48.75	116	8.54	4301	979493.70	1.33	9.65	-137.02	-127.69
1930	36	48.48	116	9.17	4377	979488.19	1.81	11.67	-137.13	-127.65
1931	36	48.18	116	8.98	4509	979480.66	2.24	16.99	-135.90	-126.17
1932	36	48.33	116	8.04	4506	979478.34	2.11	14.17	-138.75	-129.01
1933	36	48.43	116	7.73	4357	979488.53	2.12	10.21	-137.60	-128.19
1942	36	50.52	116	8.16	4436	979481.91	1.37	7.99	-143.27	-133.64
1943	36	50.53	116	7.73	4308	979490.08	1.18	4.11	-142.95	-133.59
1967	36	47.20	116	11.97	4213	979494.07	1.55	3.99	-139.45	-130.32
1968	36	47.18	116	12.65	3921	979506.76	1.32	-10.75	-144.41	-135.90
1969	36	46.50	116	13.72	3759	979514.45	1.17	-17.30	-145.55	-137.39
1970	36	46.22	116	14.12	3648	979521.89	1.14	-19.89	-144.37	-136.44
1971	36	45.45	116	12.75	4812	979443.93	7.14	12.69	-145.68	-135.60
1972	36	45.38	116	13.27	4270	979481.42	4.49	-0.67	-143.13	-134.06
1973	36	45.13	116	13.58	4208	979484.10	4.23	-3.46	-144.05	-135.10
1974	36	45.46	116	14.17	3684	979519.21	1.15	-18.09	-143.79	-135.79
bm01	36	48.48	116	11.05	4154	979503.24	1.06	5.79	-136.13	-127.09
bm02	36	48.23	116	11.77	4053	979503.95	1.05	-2.66	-141.11	-132.30

STAT NAME	LAT deg	min	LONG deg	min	ELEV feet	OG mGal	TC mGal	FAA mGal	CBA1 2.67	CBA2 2.50
s-01	36	49.82	116	9.75	4912	979456.28	2.79	28.10	-138.03	-127.45
s-02	36	49.81	116	9.85	4945	979454.07	3.03	29.06	-137.99	-127.35
sm01	36	46.21	116	14.16	3649	979520.85	1.13	-20.80	-145.32	-137.39
sm02	36	46.48	116	13.81	3740	979515.93	1.15	-17.57	-145.19	-137.06
sm03	36	46.43	116	13.44	3855	979509.51	1.37	-13.12	-144.47	-136.10
sm04	36	46.37	116	13.07	3982	979502.15	1.65	-8.41	-143.85	-135.22
sm05	36	46.53	116	12.89	4029	979499.26	1.66	-7.12	-144.15	-135.43
sm06	36	46.73	116	13.04	3921	979505.64	1.40	-11.18	-144.77	-136.26
sm08	36	46.89	116	13.19	3859	979509.10	1.23	-13.77	-145.41	-137.03
sm09	36	47.92	116	11.97	4029	979503.41	1.11	-5.05	-142.60	-133.84
sm10	36	47.42	116	12.34	4011	979502.78	1.28	-6.64	-143.41	-134.70
sm11	36	47.22	116	12.33	4062	979499.78	1.45	-4.55	-142.91	-134.10
sm12	36	47.23	116	11.46	4366	979487.38	2.05	11.61	-136.56	-127.12
sm13	36	47.47	116	11.64	4225	979495.37	1.65	6.07	-137.70	-128.54
sm14	36	47.67	116	11.60	4140	979501.93	1.42	4.27	-136.78	-127.80
sm15	36	47.93	116	10.87	4270	979496.08	1.30	10.30	-135.33	-126.06
sm16	36	47.58	116	11.17	4293	979493.53	1.69	10.46	-135.59	-126.30
sm18	36	47.23	116	13.06	3845	979510.80	1.12	-13.92	-145.16	-136.81
sm19	36	46.99	116	12.60	3991	979503.01	1.46	-7.65	-143.56	-134.90
sm20	36	46.80	116	12.26	4137	979496.79	1.91	0.17	-140.31	-131.37
sm21	36	46.72	116	12.15	4210	979493.70	2.12	4.01	-138.75	-129.66
w4e1	36	48.82	116	10.01	4324	979493.74	1.06	11.73	-136.00	-126.59
w4n1	36	48.84	116	10.02	4334	979493.20	1.07	12.08	-135.97	-126.55
w4n2	36	48.85	116	10.02	4341	979492.71	1.07	12.25	-136.05	-126.60
w4s1	36	48.80	116	10.03	4321	979494.03	1.07	11.74	-135.86	-126.46
w4s2	36	48.78	116	10.03	4315	979494.30	1.08	11.55	-135.86	-126.47
w4s3	36	48.76	116	10.04	4309	979493.71	1.08	10.35	-136.83	-127.46
w4w1	36	48.82	116	10.03	4326	979493.59	1.05	11.76	-136.04	-126.63
wf01	36	48.70	116	9.57	4303	979493.62	1.03	9.83	-137.21	-127.85
wf02	36	49.08	116	10.00	4447	979485.82	1.21	15.03	-136.77	-127.11
wf03	36	49.06	116	9.96	4438	979486.19	1.19	14.61	-136.91	-127.26
wf04	36	49.13	116	10.15	4516	979481.13	1.48	16.75	-137.14	-127.34
wf05	36	49.01	116	10.23	4441	979486.14	1.28	14.86	-136.66	-127.01
wf06	36	48.87	116	10.28	4347	979492.12	1.09	12.21	-136.27	-126.82
wf07	36	48.70	116	10.32	4282	979495.86	1.15	10.06	-136.13	-126.82
wf08	36	48.61	116	10.50	4241	979498.20	1.05	8.72	-136.18	-126.95
wf09	36	48.59	116	10.65	4227	979499.28	1.04	8.55	-135.89	-126.70
wf10	36	48.75	116	10.07	4297	979495.34	1.06	10.87	-135.92	-126.57
wf11	36	48.78	116	9.86	4320	979493.42	1.05	11.11	-136.49	-127.09
wf13	36	49.48	116	10.12	4656	979473.01	1.71	21.24	-137.20	-127.11
wf14	36	49.30	116	10.13	4558	979479.15	1.32	18.49	-137.01	-127.11
wf15	36	49.52	116	10.41	4593	979476.20	1.54	18.51	-137.97	-128.01
wf16	36	49.30	116	10.42	4495	979482.86	1.26	16.24	-137.15	-127.39
wf17	36	49.06	116	10.47	4436	979486.42	1.36	14.58	-136.68	-127.05
wf18	36	48.88	116	10.43	4347	979492.17	1.17	12.25	-136.16	-126.71

STAT NAME	LAT deg	min	LONG deg	min	ELEV feet	OG mGal	TC mGal	FAA mGal	CBA1 2.67	CBA2 2.50
wf19	36	48.72	116	10.53	4274	979496.65	1.30	10.09	-135.68	-126.40
wf20	36	48.72	116	10.78	4251	979498.99	1.05	10.28	-134.96	-125.71
wf21	36	48.93	116	10.76	4320	979493.59	1.05	11.03	-136.56	-127.17
wf22	36	49.26	116	10.68	4439	979485.98	1.15	14.17	-137.41	-127.76
wf23	36	49.41	116	10.71	4482	979482.81	1.21	14.80	-138.18	-128.44
wf24	36	49.64	116	10.52	4603	979475.10	1.44	18.12	-138.78	-128.79
wf25	36	48.83	116	10.60	4305	979494.20	1.04	10.40	-136.69	-127.32
wf26	36	48.81	116	12.02	4144	979496.37	0.96	-2.55	-144.20	-135.18
wf27	36	48.95	116	11.92	4186	979494.83	1.04	-0.29	-143.32	-134.22
wf28	36	48.91	116	11.68	4205	979495.56	0.97	2.28	-141.46	-132.31
wf29	36	48.77	116	11.76	4164	979497.83	0.96	0.87	-141.47	-132.41
wf30	36	49.11	116	11.57	4255	979494.73	1.01	5.79	-139.61	-130.35
wf31	36	48.71	116	11.57	4174	979496.19	0.97	0.21	-142.45	-133.36
wf32	36	48.92	116	11.44	4237	979496.03	1.00	5.74	-139.07	-129.85
wf33	36	49.08	116	11.37	4280	979493.26	1.01	6.71	-139.54	-130.23
wf34	36	49.21	116	11.27	4330	979490.58	1.04	8.60	-139.36	-129.94
wf35	36	48.86	116	11.13	4266	979495.92	1.03	8.45	-137.34	-128.06
wf36	36	49.48	116	11.58	4354	979486.26	1.17	6.18	-142.49	-133.02
wf37	36	49.32	116	11.47	4312	979490.05	1.04	6.23	-141.12	-131.74
wf38	36	49.55	116	11.37	4377	979485.95	1.08	7.84	-141.67	-132.15
wf39	36	49.64	116	11.15	4447	979482.45	1.13	10.86	-141.03	-131.36
wf40	36	49.64	116	10.78	4538	979478.43	1.28	15.33	-139.50	-129.64
wf41	36	49.34	116	10.93	4425	979485.69	1.18	12.45	-138.63	-129.01
wf42	36	49.09	116	10.89	4354	979490.18	1.07	10.66	-138.11	-128.63
wf43	36	48.99	116	11.07	4307	979493.34	0.99	9.49	-137.72	-128.35
wf44	36	48.98	116	11.23	4282	979494.22	1.01	8.07	-138.27	-128.95
wf45	36	49.26	116	11.14	4361	979488.80	1.05	9.68	-139.33	-129.84
wf46	36	49.50	116	10.97	4455	979483.29	1.17	12.61	-139.50	-129.81
wg02	36	48.47	116	11.25	4144	979503.29	1.03	4.87	-136.72	-127.70
wg03	36	48.55	116	11.53	4144	979502.07	1.07	3.55	-138.00	-128.99
wg04	36	48.52	116	11.86	4100	979499.35	1.08	-3.27	-143.31	-134.39
wg05	36	48.52	116	11.68	4122	979501.34	1.14	0.80	-139.93	-130.97
wg06	36	48.57	116	11.76	4120	979499.12	1.17	-1.68	-142.31	-133.36
wg07	36	48.61	116	11.89	4114	979498.36	1.03	-3.06	-143.63	-134.68
wg08	36	48.63	116	12.00	4107	979498.20	0.95	-3.91	-144.32	-135.38
wg09	36	48.65	116	12.10	4100	979497.48	0.94	-5.32	-145.49	-136.57
wg10	36	48.72	116	12.19	4099	979496.88	0.93	-6.11	-146.26	-137.34
wg11	36	48.78	116	12.28	4094	979496.55	0.95	-7.00	-146.96	-138.05
wg12	36	48.86	116	12.36	4088	979496.40	0.97	-7.83	-147.57	-138.67
wg13	36	48.90	116	12.42	4075	979497.06	0.99	-8.45	-147.72	-138.85
wg14	36	48.98	116	12.49	4083	979496.35	0.99	-8.52	-148.07	-139.18
wg15	36	49.04	116	12.57	4086	979496.13	0.98	-8.55	-148.20	-139.31
wg16	36	49.08	116	12.60	4088	979496.00	0.99	-8.55	-148.26	-139.37
wg17	36	49.11	116	12.69	4089	979495.90	0.99	-8.60	-148.35	-139.45
wg18	36	49.16	116	12.76	4090	979495.74	0.99	-8.74	-148.52	-139.62

STAT NAME	LAT deg	min	LONG deg	min	ELEV feet	OG mGal	TC mGal	FAA mGal	CBA1 2.67	CBA2 2.50
wg19	36	49.20	116	12.85	4084	979495.99	1.00	-9.11	-148.67	-139.79
wg20	36	49.24	116	12.92	4086	979495.81	1.01	-9.16	-148.79	-139.90
wl01	36	48.92	116	9.16	4316	979492.77	1.01	9.85	-137.65	-128.26
wl02	36	49.01	116	9.02	4306	979493.52	1.04	9.53	-137.59	-128.22
wl03	36	49.13	116	8.78	4295	979493.59	0.99	8.46	-138.36	-129.01
wl04	36	49.21	116	8.65	4293	979493.36	0.98	7.90	-138.85	-129.51
wl05	36	49.29	116	8.48	4290	979493.26	0.95	7.37	-139.30	-129.96
wl06	36	49.34	116	8.44	4299	979492.58	0.95	7.50	-139.49	-130.13
wl07	36	50.87	116	8.91	4793	979463.22	1.86	22.38	-140.63	-130.25
wl08	36	50.88	116	8.82	4747	979465.95	1.64	20.75	-140.89	-130.60
wl09	36	50.90	116	8.75	4715	979466.66	1.56	18.45	-142.19	-131.96
wl10	36	50.91	116	8.66	4688	979467.61	1.48	16.85	-142.95	-132.77
wl11	36	50.91	116	8.62	4670	979468.43	1.49	15.92	-143.23	-133.09
wl12	36	50.87	116	8.97	4867	979458.19	2.27	24.27	-140.84	-130.33
wl13	36	49.95	116	8.10	4350	979487.77	0.96	6.59	-142.13	-132.66
wm01	36	49.08	116	9.99	4444	979485.78	1.18	14.73	-137.01	-127.35
wm02	36	48.98	116	9.97	4396	979488.99	1.12	13.55	-136.60	-127.04
wm03	36	48.91	116	10.00	4364	979491.11	1.06	12.73	-136.36	-126.87
wm04	36	48.82	116	10.03	4326	979493.69	1.05	11.88	-135.93	-126.52
wm05	36	48.75	116	10.05	4298	979495.20	1.04	10.82	-136.02	-126.67
wm06	36	48.68	116	10.02	4272	979496.58	1.10	9.87	-136.03	-126.74
wm07	36	48.57	116	10.09	4271	979496.53	1.07	9.91	-135.99	-126.70
wm08	36	48.48	116	10.08	4278	979496.00	1.08	10.20	-135.94	-126.64
wm09	36	48.39	116	10.10	4291	979494.81	1.12	10.36	-136.19	-126.86
wm10	36	48.32	116	10.13	4297	979494.68	1.14	10.85	-135.86	-126.52
wm11	36	48.24	116	10.14	4309	979493.77	1.20	11.19	-135.88	-126.52
wm12	36	48.16	116	10.16	4320	979492.95	1.23	11.53	-135.88	-126.50
wm13	36	48.08	116	10.19	4349	979491.23	1.30	12.65	-135.69	-126.25
wm14	36	47.90	116	10.23	4418	979486.99	1.60	15.16	-135.25	-125.68
wm15	36	47.78	116	10.24	4461	979484.31	1.68	16.70	-135.11	-125.44
wm16	36	49.17	116	10.02	4486	979483.16	1.26	15.93	-137.16	-127.41
wm17	36	49.23	116	10.04	4543	979479.77	1.67	17.74	-136.87	-127.03
wm18	36	49.27	116	10.07	4635	979473.45	2.21	20.01	-137.22	-127.21
wm19	36	49.30	116	10.00	4571	979478.18	1.39	18.68	-137.17	-127.24
wm20	36	49.39	116	9.98	4628	979474.88	1.50	20.66	-137.05	-127.01
wr01	36	48.78	116	10.97	4251	979497.29	1.05	8.50	-136.74	-127.49
wr02	36	48.27	116	10.82	4215	979499.87	1.13	8.43	-135.49	-126.33
wr03	36	48.15	116	11.20	4168	979501.95	1.14	6.27	-136.04	-126.98
wr04	36	47.70	116	10.63	4399	979487.23	1.79	13.91	-135.66	-126.14
ws-b	36	49.81	116	9.67	4896	979457.17	2.88	27.54	-137.97	-127.43
ws-d	36	48.95	116	9.09	4309	979493.41	1.01	9.83	-137.45	-128.07
ws01	36	48.85	116	9.29	4320	979492.68	1.00	10.26	-137.38	-127.98
ws02	36	49.79	116	9.61	4843	979460.87	2.53	26.23	-137.79	-127.35
ws03	36	49.84	116	9.57	4838	979461.20	2.48	26.06	-137.86	-127.43
ws04	36	49.83	116	9.60	4831	979461.89	2.42	26.14	-137.61	-127.19

STAT NAME	LAT deg	min	LONG deg	min	ELEV feet	OG mGal	TC mGal	FAA mGal	CBA1 2.67	CBA2 2.50
ws05	36	49.81	116	9.46	4726	979468.47	1.90	22.81	-137.84	-127.61
ws06	36	49.81	116	9.38	4688	979470.76	1.76	21.53	-137.96	-127.80
ws07	36	49.81	116	9.30	4644	979473.06	1.60	19.68	-138.46	-128.39
ws08	36	49.80	116	9.23	4621	979473.41	1.51	17.95	-139.52	-129.49
ws09	36	49.80	116	9.17	4601	979474.47	1.45	17.13	-139.71	-129.73
ws10	36	49.80	116	9.09	4572	979476.53	1.38	16.42	-139.48	-129.55
ws11	36	49.80	116	9.03	4546	979478.14	1.33	15.62	-139.46	-129.58
ws12	36	49.81	116	8.94	4519	979480.22	1.27	15.11	-139.08	-129.27
ws13	36	49.80	116	8.86	4481	979482.46	1.18	13.84	-139.16	-129.41
ws14	36	49.79	116	8.79	4464	979483.36	1.14	13.17	-139.29	-129.59
ws15	36	49.79	116	8.71	4451	979483.46	1.11	11.98	-140.04	-130.36
ws16	36	49.79	116	8.63	4435	979484.14	1.09	11.14	-140.35	-130.71
ws17	36	49.80	116	8.54	4416	979485.26	1.05	10.49	-140.40	-130.79
ws18	36	49.79	116	8.25	4352	979488.66	0.99	7.87	-140.88	-131.41
ws19	36	49.79	116	7.95	4292	979491.24	0.94	4.83	-141.92	-132.58